AD NUMBER: AD0810815

LIMITATION CHANGES

TO:

Approved for public release; distribution is unlimited.

FROM:

Distribution authorized to US Government Agencies and Contractors only; Administrative/Operational Use; 2 Aug 1967. Other requests shall be referred to Office of Naval Research, Arlington, VA 22203

AUTHORITY

USNRL ltr dtd 2 Aug 1971

LUMPED PARAMETER BEAM MODELS BASED ON MECHANICAL IMPEDANCE

by

Vernon H. Neubert

and

Hae Lee

Department of Engineering Mechanics
The Pennsylvania State University

Office of Naval Research
Contract No. Nonr-656(28)(X)
Interim Report No. 6

February 1967

TABLE OF CONTENTS

Lumped Parameter Beam Models Based on Mechanical Impedance

Introduction

A new method has been used to derive lumped parameter beam and bar elements which represent accurately the dynamic response of a beam or bar having uniformly distributed mass. Although a general approach suitable for various inputs has been devised, the dynamic loading of greatest interest is assumed to be translational ground shock. The present report summarizes all the approaches that have been developed and published during the past several years, but emphasizes the impedance method, which is demonstrated to be most promising.

The approaches used are based on the idea of improving the accuracy of stresses and deflections predicted using lumped parameter models by developing better basic elements. The lumped parameter models are developed so that certain parameters in the equations for the dynamic response of the model will be exactly the same as those for the simulated uniform bar or beam.

Since the input of primary concern is ground shock, some of the first work involved making the natural frequencies, shock effective mass (or shear factor) and shock effective inertia (or moment factor) accurate. Some results of this work are summarized in Appendix C and in published reports.[1,2] Although the approach has the advantage that the important parameters are directly involved, it was found that the response of combinations of the elements was not necessarily improved.

The method that has been most fruitful is based on the concept of making the impedance at the ends of the bar and beam segments

accurate. The general mobility approach and results of application to bars was published in references 2 and 3, and is summarized in Appendix B. The impedance approach to beams was recorded in references 4 and 5, with application to a clamped-propped beam. The impedance method is summarized in the main body of this report, and models are indicated for the clamped-clamped beam. Results for other boundary conditions are summarized in Appendix A.

Background

It can be readily shown that if several linear, elastic bodies are to be connected, the impedance of the interconnected system may be predicted if appropriate impedances of the separate bodies are known. Points at which impedances must be determined are connection points and load points. Since bodies may be further subdivided at load points, the problem can be reduced to the determination of impedances only at connection points.

Thus the idea of developing lumped parameter elements which adequately represent boundary impedance of beam segments has a firm mathematical basis. Through Fourier transform techniques it can also be demonstrated that if the lumped parameter model accurately represents impedance characteristics in a certain frequency range, it will also adequately represent transient response, if the Fourier transform of the forcing function is limited to the same frequency range.

Impedance here is defined as force or moment due to displacement or rotation which vary as sinusoidal functions of time. The difference between impedance and mobility is the same as the difference between stiffness and flexibility in static

problems. To find terms in an impedance matrix, only one point is allowed to move while the others are held fixed against translation or rotation. Thus, the clamped-clamped beam perturbed at the supports is the most basic element in the impedance approach, and is discussed in detail. Results for beam elements with other boundary conditions are summarized in Appendix A.

Clamped-Clamped Beam

The sign convention is indicated in Figure 1(a). For the Bernoulli-Euler beam with uniformly distributed mass, the relationship between forces {F} and displacements {w} at the beam ends is given by

$$\{w\} = [Z]\{F\} \tag{1}$$

or

$$\begin{Bmatrix} w_o \\ \phi_o \\ \phi_l \\ w_l \end{Bmatrix} = \begin{bmatrix} & Z_{ij} & \end{bmatrix} \begin{Bmatrix} V_o \\ M_o \\ M_l \\ V_l \end{Bmatrix} \tag{2}$$

The impedance matrix Z_{ij} is given exactly by:

$$[Z_{ij}] = \frac{EI}{\ell^3} \times \frac{(\beta\ell)^3}{(1-\text{Cos } \beta\ell \text{ Cosh } \beta\ell)}$$

$$\begin{bmatrix} (Ch\cdot S+C\cdot Sh) & \beta^{-1}(Sh\cdot S) & \beta^{-1}(Ch-C) & -(Sh+S) \\ \beta^{-1}(Sh\cdot S) & \beta^{-2}(Ch\cdot S-Sh\cdot C) & \beta^{-2}(Sh-S) & -\beta^{-1}(Ch-C) \\ \beta^{-1}(Ch-C) & \beta^{-2}(Sh-S) & \beta^{-2}(Ch\cdot S-Sh\cdot C) & -\beta^{-1}(Sh\cdot S) \\ -(Sh+S) & -\beta^{-1}(Ch-C) & -\beta^{-1}(Sh\cdot S) & (Ch\cdot S+C\cdot Sh) \end{bmatrix} \tag{3}$$

By virtue of Maxwell's reciprocal theorem and symmetry, the matrix is symmetric about both the major and minor diagonal, so there are only six original elements in Eq. (3). These are, for example, Z_{11}, Z_{22}, Z_{12}, Z_{13}, Z_{23}, Z_{14}.

The form of the lumped-parameter model developed is shown in Fig. 1(b). It is symmetric and carries two intermediate masses m_1 and two end masses m_2. The sum $2(m_1 + m_2) = \mu\ell$, the total mass of the beam, or if $m_1 = \alpha\mu\ell$, then $m_2 = (0.5 - \alpha)\mu\ell$. The distance of m_1 from the support is $\xi\ell$. There are then two parameters to be determined: α and ξ. The six impedances for the lumped parameter system in terms of α, ξ, EI, β and ℓ are given in Table I.

The expressions of Z_{ij} from Table 1 are equated to the corresponding expressions in Equation (3), and the values of α and ξ determined which lie in the region $0 < \alpha < 0.5$ and $0 < \xi < 0.5$ when $\beta\ell$ is varied. Since there is one equation associated with each Z_{ij} and two unknowns, the equations are solved by choosing a value for ξ and determining the resulting value of α. Results are shown in Figure 2.

As seen in Figure 2, there are two separate regions of promise for a model. Point A($\xi = 0.284$, $\alpha = 0.408$) is common to the curves for $\frac{M_o}{w_o}$, $\frac{V_1}{w_o}$, and $\frac{V_o}{w_o}$ and is near to $\frac{M_1}{w_o}$. Point B($\xi = 0.311$, $\alpha = 0.364$) is approximately common to all curves but that for $\frac{M_o}{w_o} = Z_{12}$.

Since the bending moment introduced due to translation is important, the model designated OP2 is based on Point A. The model CG2 has center of gravity positioning with $\xi = 0.333$ and $\alpha = 0.333$. When two OP2 models are connected, the combination is designated OP6.

Comparison of Transient Response

The accuracy of the representation of the impedance Z_{ij} is directly related to the accuracy of the transient response. The impedance expressions of Eq. (3) may be expanded in a power series in terms of $\beta\ell$, to indicate their variation at low frequencies, namely:

$$Z_{ij} = \frac{EI}{\ell^3} \left[a_o + a_1(\beta\ell)^4 + a_2(\beta\ell)^8 + \ldots \right] \qquad (4)$$

As shown in reference 4, the a_o coefficients are the elements in the static stiffness matrix and the a_1 coefficients are the elements in the non-diagonal inertia matrix suggested by Archer[9] and Leckie and Lindberg.[10] Thus, if a model could be developed in which the a_2 coefficients were also accurate, this would represent an improvement over existing techniques and would have the advantage of being associated with a physical system.

The coefficients a_i of the power series for impedances of various models are shown in Table II(a). Comparison shows that the OP2 model is superior to the CG model for Z_{11}, Z_{12} and Z_{14} as expected. The values for a model OP2B based on Point B are also given.

Natural frequencies, shock effective mass, and shock effective inertia or bending factor (see Appendix C or Reference 11 for definition) are given in Tables III, IV and V. As is seen in III, CG models give better values for natural frequencies than OP models. There is no consistent trend in the models regarding shock effective mass and bending effective factor.

Now suppose the various models are submitted to a transient input in the form of a translational, half-sine, ground acceleration, namely,

$$\ddot{s}(t) = A_o \sin \frac{\pi t}{\tau} \qquad 0 \leq t \leq \tau$$
$$= 0 \qquad t \geq \tau \tag{5}$$

Then the normal mode solution for the shear force and bending moment at the clamped end becomes

$$V(0,t) = 8\mu\pi A_o \sum_{n=1,3,5}^{\infty} \frac{\alpha_n^2}{(\beta_n \ell)^2} R_n(t) \tag{6}$$

$$M(0,t) = -8\mu\ell^2 A_o \sum_{n=1,3,5}^{\infty} \frac{\alpha_n}{(\beta_n \ell)^3} R_n(t) \tag{7}$$

where α_n and $\beta_n \ell$ are the same values tabulated by Young and Felgar,[8] and

$$R_n(t) = \left[\sin \frac{\pi t}{\tau} - \frac{\pi}{\omega_n \tau} \sin \omega_n t\right] \left[1 - \frac{\pi^2}{\omega_n^2 \tau^2}\right]^{-1} \qquad 0 \leq t \leq \tau \tag{8}$$

$$R_n(t) = -\frac{\pi}{\omega_n \tau} \left[\sin \omega_n t + \sin \omega_n (t-\tau)\right] \left[1 - \frac{\pi^2}{\omega_n^2 \tau^2}\right]^{-1} \qquad t \geq \tau \tag{9}$$

$$\beta_n^4 \ell^4 = \frac{\mu \omega_n^2 \ell^4}{EI} \qquad \text{or} \qquad \omega_n = \beta_n^2 \ell^2 \sqrt{\frac{EI}{\mu \ell^4}} \tag{10}$$

Note that $\sqrt{\frac{EI}{\mu \ell^4}}\, t$ is a non-dimensional time.

The half-sine input has a Fourier spectrum with relatively little content for $\omega_c \tau / \pi > 3$, so ω_c might be called a cut-off frequency. If $\omega_c = \frac{3\pi}{\tau} = \beta_c^2 \ell^2 \sqrt{\frac{EI}{\mu \ell^4}} = 15 \sqrt{\frac{EI}{\mu \ell^4}}$, then the cut-off value is $\beta_c \ell = \sqrt{15}$ = 3.87. This case is plotted in Figs. 3&4. Note that for a clamped-clamped beam the value of $\beta_n \ell$ for n=1 is 4.73. An input with $\beta_c \ell = 1.73$ is also considered. (Figs. 5 & 6).

Summary and Conclusions

The impedance method is demonstrated to yield beam models that represent the low frequency shock response more accurately than center-of-gravity type models. In addition, the error may be anticipated from the Fourier integral relationship of the type:

$$x(t) = \frac{1}{2\pi} \int_{-\infty}^{\infty} H(\omega)F(\omega)e^{i\omega t}d\omega$$

Models suitable for practical analysis are developed for the clamped-clamped beam and, in Appendix A, for other beam boundary conditions.

For the clamped-clamped beam there are six elements in the 4 x 4 impedance matrix to be matched. With two parameters available, five elements are matched fairly well. It therefore appears worthwhile to consider using a model with three parameters.

The impedance method lends itself to development of accurate elements in any frequency range. The power series would be expanded about some frequency other than zero and model parameters chosen for matching.

The examples, and the basic theory, show that if all the impedances are accurate at the boundaries for a simple model, combinations of the simple models will also be accurate.

Table I

Impedances of Lumped Model

$$\frac{EI\Delta}{\ell^3} = \frac{1}{12} - \alpha\xi^3(1-\xi)^3(\beta\ell)^4/18 + \alpha^2\xi^4(\beta\ell)^8\Big[3(1-\xi)^4 + 6\xi(1-\xi)^3 - 3(1-\xi)^3 - 12\xi(1-\xi)^5 - 2\xi^2(1-2\xi)^3\Big]/432$$

$$Z_{11}\Delta = 1 - \Big\{\frac{1}{24} - \xi^2(1-\xi)^2\alpha\Big\}(\beta\ell)^4 + \Big\{\xi^3(1-\xi)^3\alpha/36 - \xi^3\alpha^2\Big[2(1-6\xi^2+6\xi^3) + 12(1-\xi)^3 - 3\xi(1-2\xi)^3 - 3(8\xi^2-11\xi+4\Big]/72\Big\}(\beta\ell)^8 + \Big\{\xi^4\alpha^2\Big[2\xi^2(1-2\xi)^3 + 12\xi(1-\xi)^5 + 3(1-2\xi)^3 - 3\xi(1-2\xi)^3 - 3(1-\xi)^4 - 3\xi(1-2\xi)^3\Big]/864 - \xi^5\alpha^3\Big[4\xi(1-2\xi)^3 + 12(1-\xi)^2(1-6\xi^2+6\xi^3) + 18(1-\xi)(1-2\xi)^3 - 12\xi(1-\xi)(1-2\xi)^3 - 6(1-\xi)^2(8\xi^2-11\xi+4) - 6(1-2\xi)^3\Big]/864\Big\}(\beta\ell)^{12}$$

$$Z_{12}\Delta = \frac{1}{2} + \alpha\xi\{-1 + 2\xi - 2\xi^2 + \xi^3\}(\beta\ell)^4/12 + \alpha^2\xi^4\{-2 + 10\xi - 15\xi^2 + 4\xi^3 + 4\xi^4\}(\beta\ell)^8/72$$

$$Z_{13}\Delta = \frac{1}{2} + \{\alpha\xi^2(1-\xi)^2/12\}(\beta\ell)^4 + \{\alpha^2\xi^5(1-2\xi)^3/72\}(\beta\ell)^8$$

$$Z_{14}\Delta = -1 + \{\alpha\xi^2(1-\xi)^2/2\}(\beta\ell)^4 - \{\alpha^2\xi^4(1-2\xi)^3/24\}(\beta\ell)^8$$

$$Z_{22}\Delta = \frac{1}{3} - \alpha\{\xi^3(1-\xi)^3/18 + \xi(1-\xi)/12 - \xi(1-3\xi+4\xi^2-2\xi^3)/12 - \xi^2(1-\xi)^2/12\}(\beta\ell)^4 - \alpha^2\xi^3\{\xi^3(1-\xi)^3 + 6\xi(1-\xi)^4 + 3(1-2\xi)^3 - 3\xi(1-2\xi)^3 - 3(1-\xi)^2(1-3\xi+4\xi^2-2\xi^3) - 3\xi^3(1-2\xi)^3\}(\beta\ell)^8/216$$

$$Z_{23}\Delta = \frac{1}{6} + \{\alpha\xi^3(1-\xi)^3/18\}(\beta\ell)^4 - \{\alpha^2\xi^6(1-2\xi)^3/216\}(\beta\ell)^8$$

Table II. Power Series Coefficients a_i, Clamped-Clamped Beam

		a_o	a_1	a_2
Z_{11}	Exact	12	-0.371428	-0.0003646
	OP2	12	-0.371338	-0.0004024
	OP2B	12	-0.371070	-0.0003778
	CG2	12	-0.372241	-0.0003563
Z_{12}	Exact	6	-0.052381	-0.0000765
	OP2	6	-0.052372	-0.0000796
	OP2B	6	-0.046959	-0.0000794
	CG2	6	-0.042940	-0.0000781
Z_{13}	Exact	6	0.030953	0.0000723
	OP2	6	0.030592	0.0000687
	OP2B	6	0.031038	0.0000724
	CG2	6	0.031023	0.0000736
Z_{14}	Exact	-12	-0.128572	-0.003298
	OP2	-12	-0.128665	-0.0003272
	OP2B	-12	-0.128929	-0.0003310
	CG2	-12	-0.127759	-0.0003268
Z_{22}	Exact	4	-0.009523	-0.0000162
	OP2	4	-0.010009	-0.0000578
	OP2B	4	-0.009551	-0.0000361
	CG2	4	-0.009524	-0.0000215
Z_{23}	Exact	2	0.007143	0.0000135
	OP2	2	0.006861	0.0000159
	OP2B	2	0.007163	0.0000150
	CG2	2	0.007298	0.0000158

Table III. Natural Frequencies, Clamped-Clamped Beam

	Uniform	OP2	CG2	OP6	CG6
$\beta_1 \ell$	4.7300	4.7359	4.7309	4.7269	4.7291
$\beta_3 \ell$	10.9956	-	-	11.3588	10.8634
$\beta_5 \ell$	17.2788	-	-	16.3847	15.2244

Table IV. Shock Effective Mass, Clamped-Clamped Beam

Mode	Uniform	OP2	CG2	OP6	CG6
I	0.3452	0.4080	0.333	0.3446	0.3449
III	0.0662	-		0.1054	0.0629
V	0.0023	-		0.0040	0.0010
Sum	0.4137	0.408	0.333	0.454	0.4088
$\sum_{n=1}^{\infty}$	0.5000				

Table V. Bending-Effective Factor, Clamped-Clamped Beam

Mode	Uniform	OP2	CG2	OP6	CG6
I	0.07300	0.0830	0.0730	0.0740	0.0743
III	0.0060	-	-	0.0090	0.0060
V	0.0002	-	-	0.0002	0.0007
Sum	0.0792	0.0830	0.0730	0.0832	0.0810
$\sum_{n=1}^{\infty}$	0.08333				

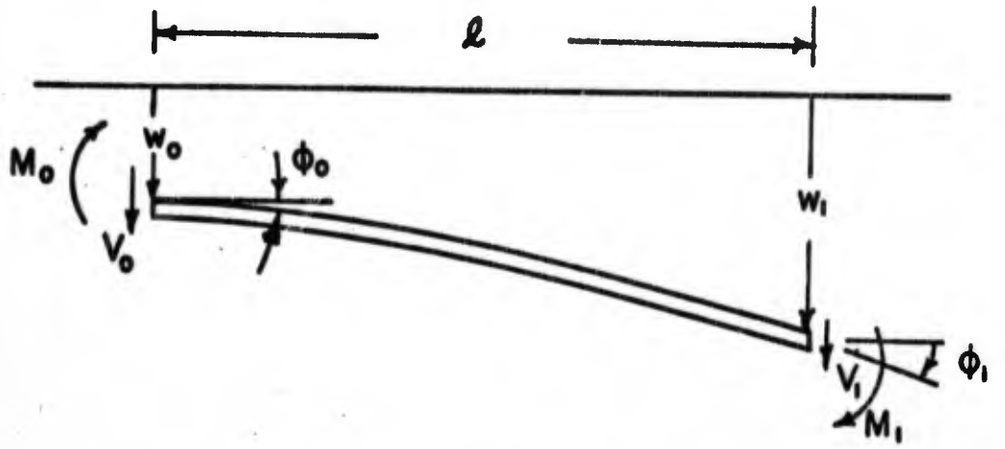

(a) UNIFORM BEAM SEGMENT AND SIGN CONVENTION

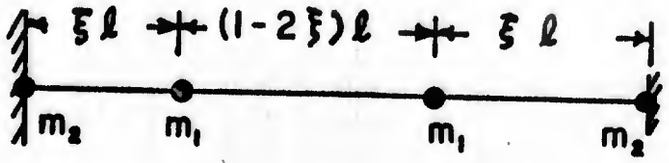

$m_1 = a\mu\ell \qquad m_2 = (0.5-a)\mu\ell$

(b) LUMPED MODEL

FIG 1

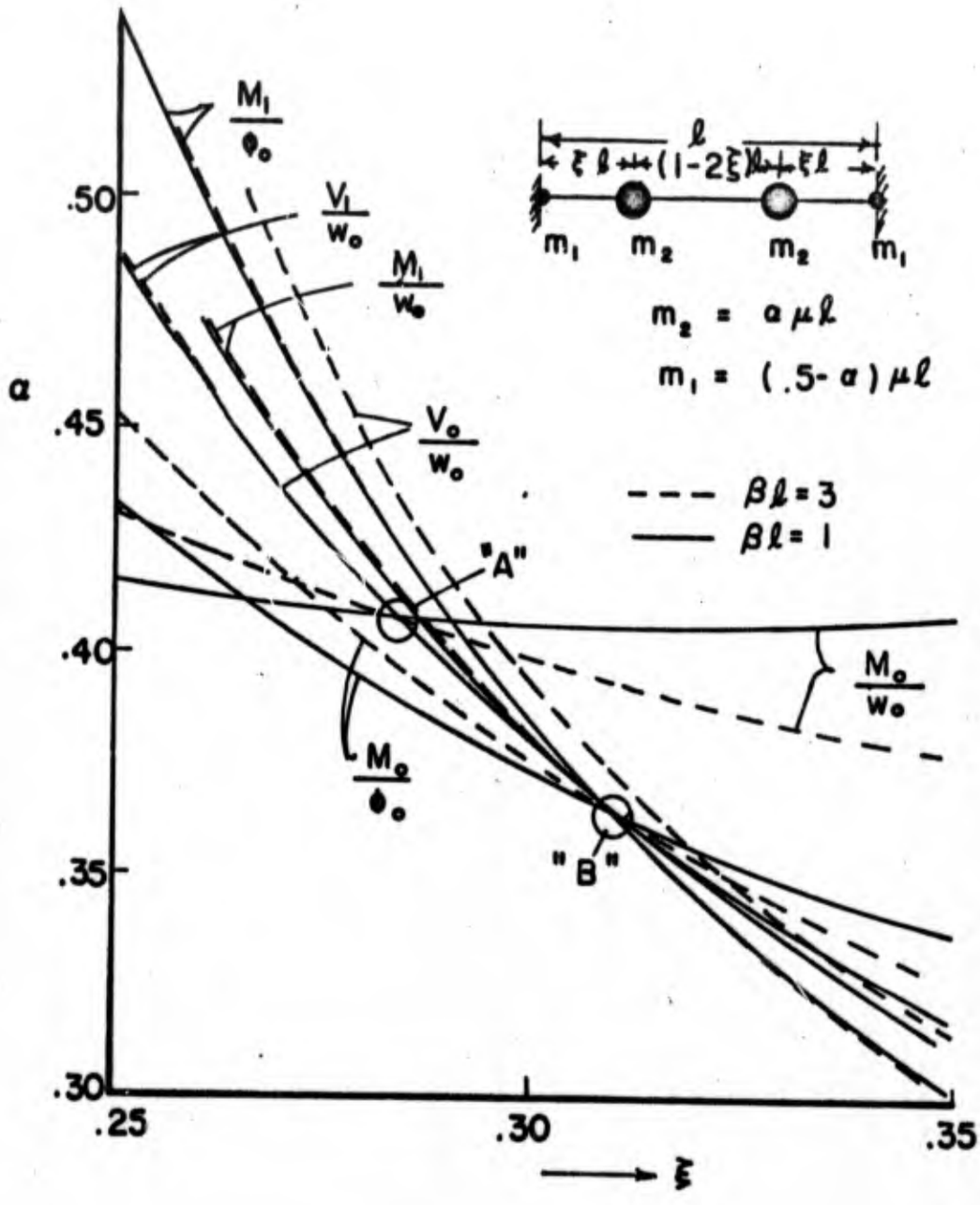

FIG. 2 OPTIMIZING CONDITION, CLAMPED-CLAMPED BEAM

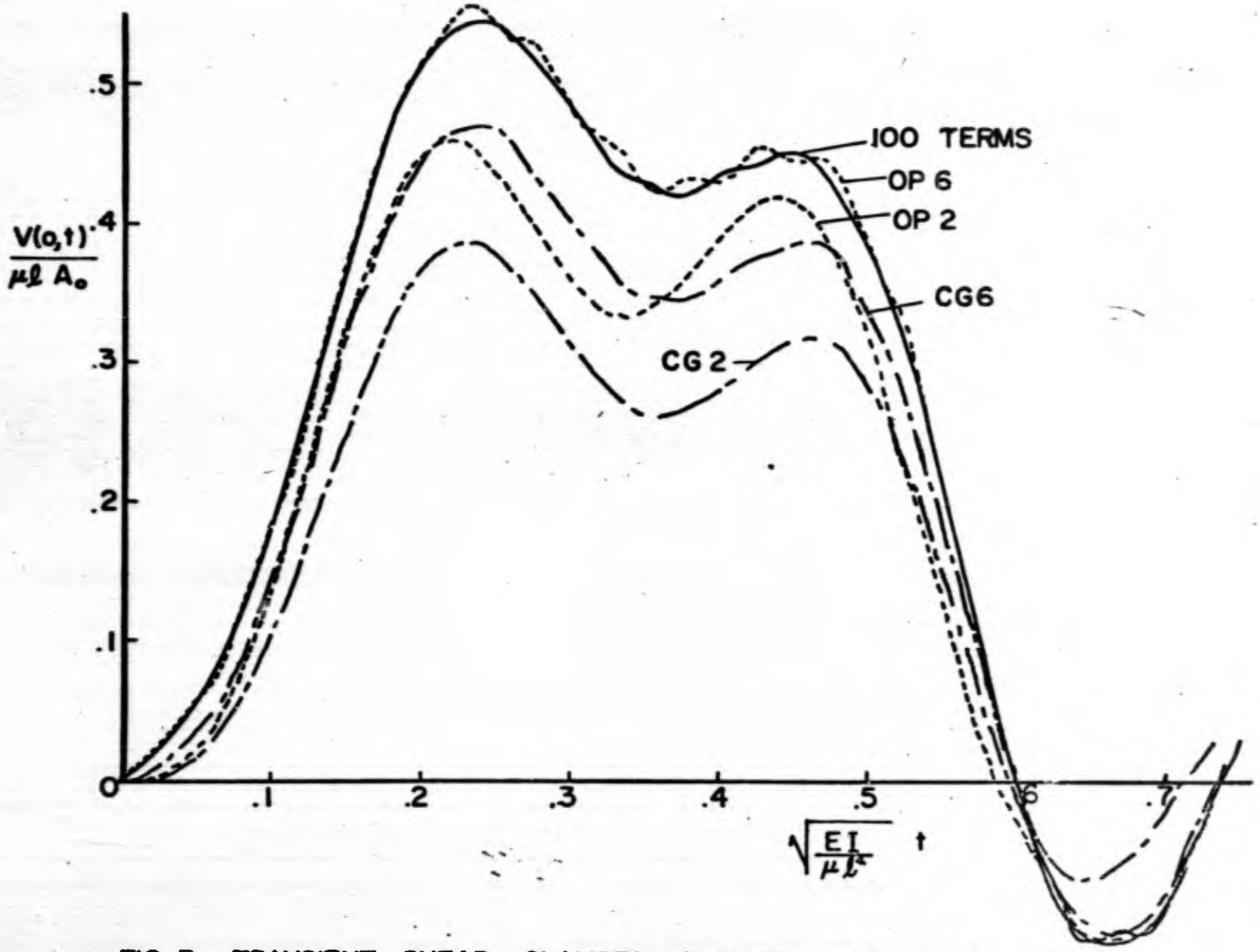

FIG. 3 TRANSIENT SHEAR , CLAMPED - CLAMPED BEAM ($\beta_c \ell = 3.87$)

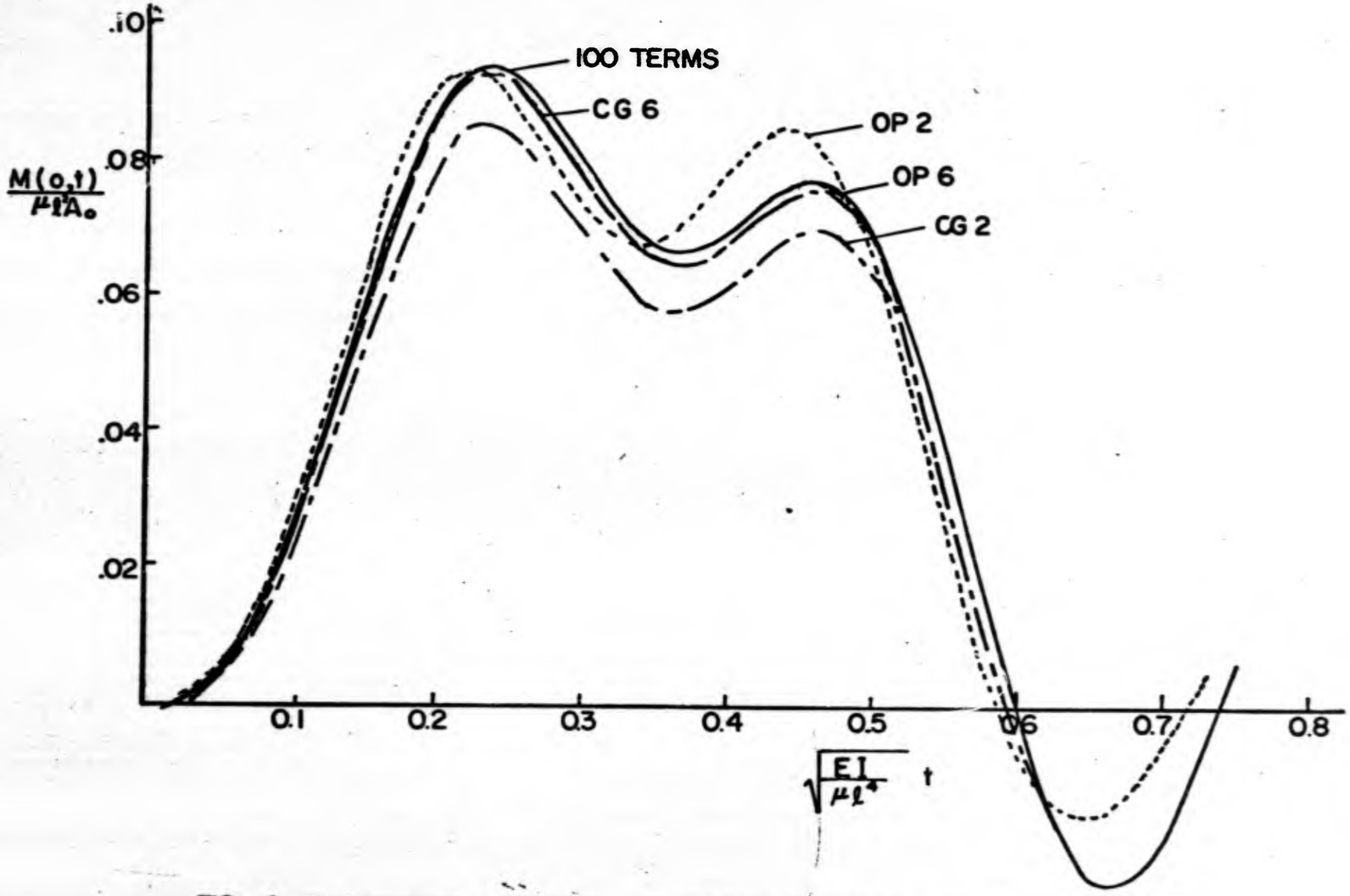

FIG. 4 TRANSIENT MOMENT, CLAMPED-CLAMPED BEAM ($\beta_c \ell = 3.87$)

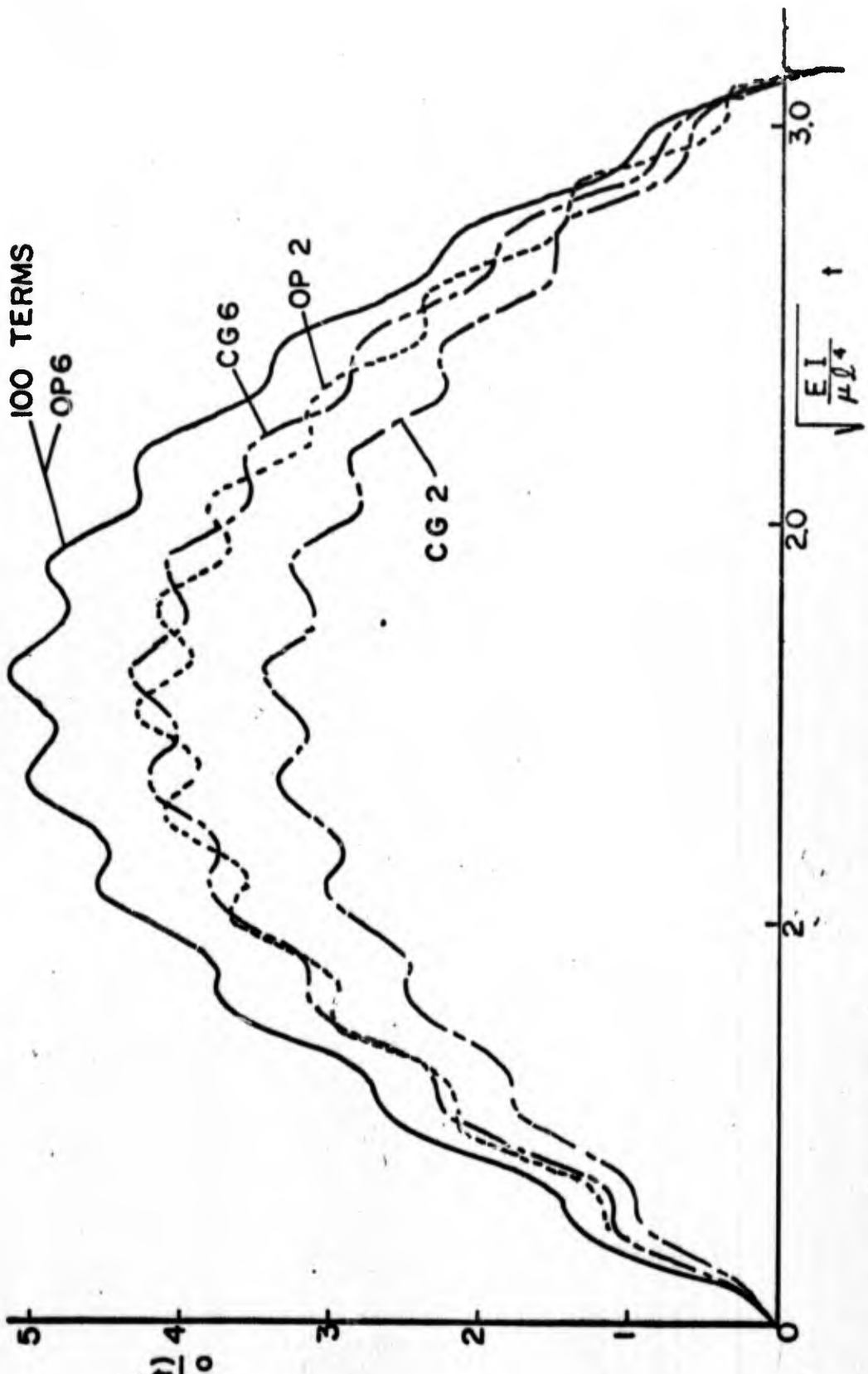

FIG. 5 TRANSIENT SHEAR, CLAMPED-CLAMPED BEAM ($\beta_c l = 1.73$)

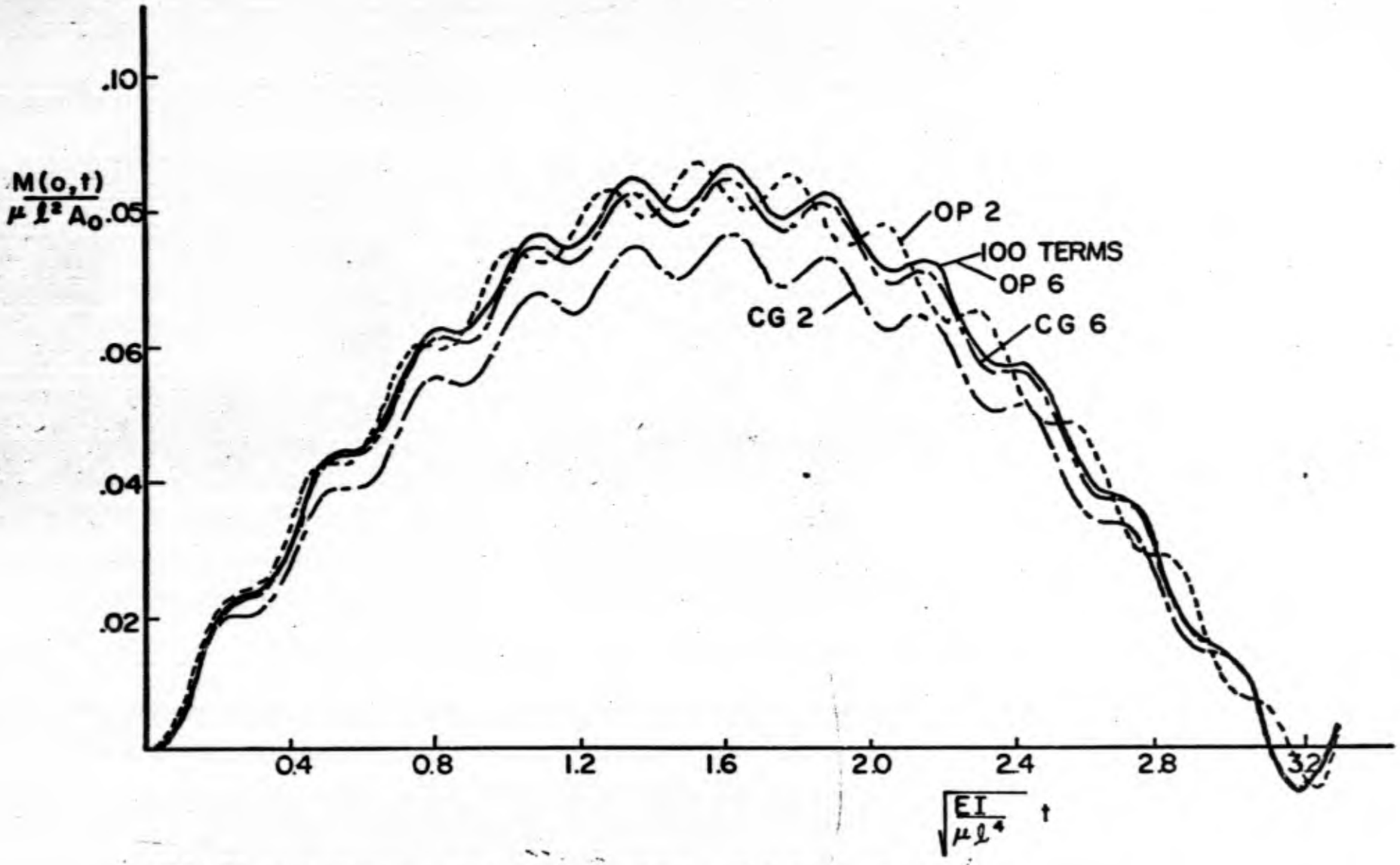

FIG. 6 TRANSIENT MOMENT, CLAMPED– CLAMPED BEAM ($\beta_c \ell = 1.73$)

Appendix A

Beam Models for Various Boundary Conditions using Impedance Methods

Theoretically, the impedance matrix for beam elements having the usual simple boundary conditions may be determined from the matrix for the clamped-clamped beam. In terms of the six basic impedances, the matrix for the clamped-clamped beam is:

$$\begin{Bmatrix} V_o \\ M_o \\ M_1 \\ V_1 \end{Bmatrix} = \begin{bmatrix} Z_{11} & Z_{12} & Z_{13} & Z_{14} \\ Z_{12} & Z_{22} & Z_{23} & -Z_{13} \\ Z_{13} & Z_{23} & Z_{22} & -Z_{12} \\ Z_{14} & -Z_{13} & -Z_{12} & Z_{11} \end{bmatrix} \begin{Bmatrix} w_o \\ \phi_o \\ \phi_1 \\ w_1 \end{Bmatrix} \qquad \text{(A-1)}$$

Hinged-Hinged Beam

For the hinged-hinged beam $M_o = M_1 = 0$. The variables ϕ_o and ϕ_1 may be related directly to w_o and w_1, and the impedance matrix for the hinged-hinged beam is then a 2 x 2 matrix.

In terms of the six impedance coefficients in (A-1), the value of $\frac{V_o}{w_o}$ for the hinged-hinged beam is

$$\frac{V_o}{w_o} = Z_{11} + \left[\frac{2Z_{13} Z_{23} Z_{12} - Z_{12}^2 Z_{22} - Z_{13}^2 Z_{22}}{Z_{22}^2 - Z_{23}^2} \right] \qquad \text{(A-2)}$$

If the actual values for the uniform beam are introduced, some cancellation occurs and identification of terms leads to:

$$\frac{V_o}{w_o} = \frac{1}{2}\left[Z_{11} + \frac{Z_{13}Z_{14}}{Z_{12}}\right] \qquad \text{(A-3)}$$

Likewise

$$\frac{V_1}{w_o} = Z \quad + \left[\frac{2Z_{13}Z_{12}Z_{22} - Z_{12}^2Z_{23} - Z_{13}^2Z_{23}}{Z_{22}^2 - Z_{33}^2}\right] \qquad \text{(A-4)}$$

and

$$\frac{V_1}{w_o} = \frac{1}{2}\left[Z_{14} + \frac{Z_{11}Z_{13}}{Z_{12}}\right] \qquad \text{(A-5)}$$

The detailed expressions are

$$\frac{V_o}{w_o} = \frac{EI(\beta\ell)^3}{\ell^3}\left[\frac{\text{Cos}\beta\ell\text{Sinh}\beta\ell - \text{Sin}\beta\ell\text{Cosh}\beta\ell}{2\text{Sin}\beta\ell\text{Sinh}\beta\ell}\right] \qquad \text{(A-6)}$$

$$\frac{V_1}{w_o} = \frac{EI(\beta\ell)^3}{\ell^3}\left[\frac{\text{Sinh}\beta\ell - \text{Sin}\beta\ell}{2\text{Sin}\beta\ell\text{Sinh}\beta\ell}\right] \qquad \text{(A-7)}$$

The moment at the centre-line is considered and is

$$\frac{M(\frac{\ell}{2})}{w_o} = \frac{EI(\beta\ell)^2}{4\ell^2}\left[\frac{\text{Cos}\,\frac{\beta\ell}{2} - \text{Cosh}\,\frac{\beta\ell}{2}}{\text{Cos}\,\frac{\beta\ell}{2}\,\text{Cosh}\,\frac{\beta\ell}{2}}\right] \qquad \text{(A-8)}$$

For the lumped model as shown in Fig. A-1, the corresponding expressions are

$$\frac{V_o}{w_o}\cdot\Delta = \left[\alpha(-1+2\xi - 2\xi^2)(\beta\ell)^4 + \alpha^2(1-5\xi + 8\xi^2 - 4\xi^3)\xi^2(\beta\ell)^8/3\right] - (\beta\ell)^4(0.5 - \alpha)\Delta \qquad (A\text{-}9)$$

$$\frac{V_1}{w_o}\cdot\Delta = \alpha(2\xi - 2\xi^2)(\beta\ell)^4 + \alpha^2\{\xi^2(1-2\xi)^3\}(\beta\ell)^8/6 \qquad (A\text{-}10)$$

$$\frac{M(\frac{\ell}{2})}{w_o}\cdot\Delta = -\alpha\xi(\beta\ell)^4/2 + \alpha^2\{4\xi^5 - 4\xi^4 + \xi^3\}(\beta\ell)^8/12 \qquad (A\text{-}11)$$

$$\Delta = 1 - \frac{2\alpha\xi^2}{3}(1-\xi)^2(\beta\ell)^4 + \alpha^2\xi^4\left[3-16\xi + 28\xi^2 - 16\xi^3\right](\beta\ell)^8/36 \qquad (A\text{-}12)$$

The values of α and ξ which make $\frac{V_o}{w_o}$ for the model and the uniform beam exactly the same for $\beta\ell = 1$ and $\beta\ell = 3$ are shown in Fig. A-1. The curve for $\frac{V_1}{w_o}$ is slightly different, but to plotting accuracy the curves are practically identical. There is a crossing sufficiently close to the point $\xi = 0.284$ and $\alpha = 0.408$ that a model was investigated for this point - which happens to be the same mass distribution and positioning as used for one of the clamped-clamped beam lumped models. The coefficients of the power series for the OP2 hinged-hinged beam models are given in Table A-I. Unfortunately Figure A-1 shows that the moment at the center-line, which is the high stress point, is not well matched by the model chosen.

Table A-I. Coefficients of Series Solution
Hinged-Hinged Beam

		a_o	a_1	a_2
$\frac{V_o}{w_o}$	Exact	0.	-0.16667	-0.00205
	OP2	0.	-0.16593	-0.00205
	CG2	0.	-0.14793	-0.00170
$\frac{V_1}{w_o}$	Exact	0.	+0.33333	+0.00212
	OP2	0.	+0.33407	+0.00212
	CG2	0.	+0.35207	+0.00172

In Figures A-2 through A-4, the impedance ratios are plotted as a function of $\beta\ell$. As expected the OP2 model represents the low frequency ratios $\frac{V_o}{w_o}$ and $\frac{V_1}{w_o}$ very well, but the moment $M(\ell/2)/w_o$ shows only slight improvement over the CG model.

Clamped-Propped Beam

In Figure A-5 the optimizing condition for a clamped-propped beam is shown as taken from References 4 and 5. Note that $L = 2\ell$ or twice the beam length. The model investigated was based on shear only, that is $Z_{44} = \frac{V_4}{w_4}$; $Z_{34} = \frac{V_3}{w_4}$; and $Z_{33} = \frac{V_3}{w_3}$. The values used are $\alpha = 0.20$ and $\xi = 0.368$. In terms of ℓ the distance from the left end to m_2 is then 0.316ℓ and the masses are: $m_3 = 0.40\mu\ell$ and $m_2 = 0.60\mu\ell$.

Clamped-Guided Beam

The optimizing condition for the clamped-guided beam is shown in Figure A-6. In this case a reasonable choice is $\alpha = .85$ and $\xi \cong .535$, based on curves for $\frac{M_o}{w_o}$ and $\frac{V_o}{w_o}$, which deal with values at the clamped end. Here the curves are for $\beta\ell = 1$ and $\beta\ell = 2$.

Clamped-Free Beam

In Figure A-7 are given curves for the clamped-free beam for $\frac{V_o}{w_o}$ and $\frac{M_o}{w_o}$. Here taking $\alpha = .83$ and $\xi = 0.61$ yields a model for low frequency response.

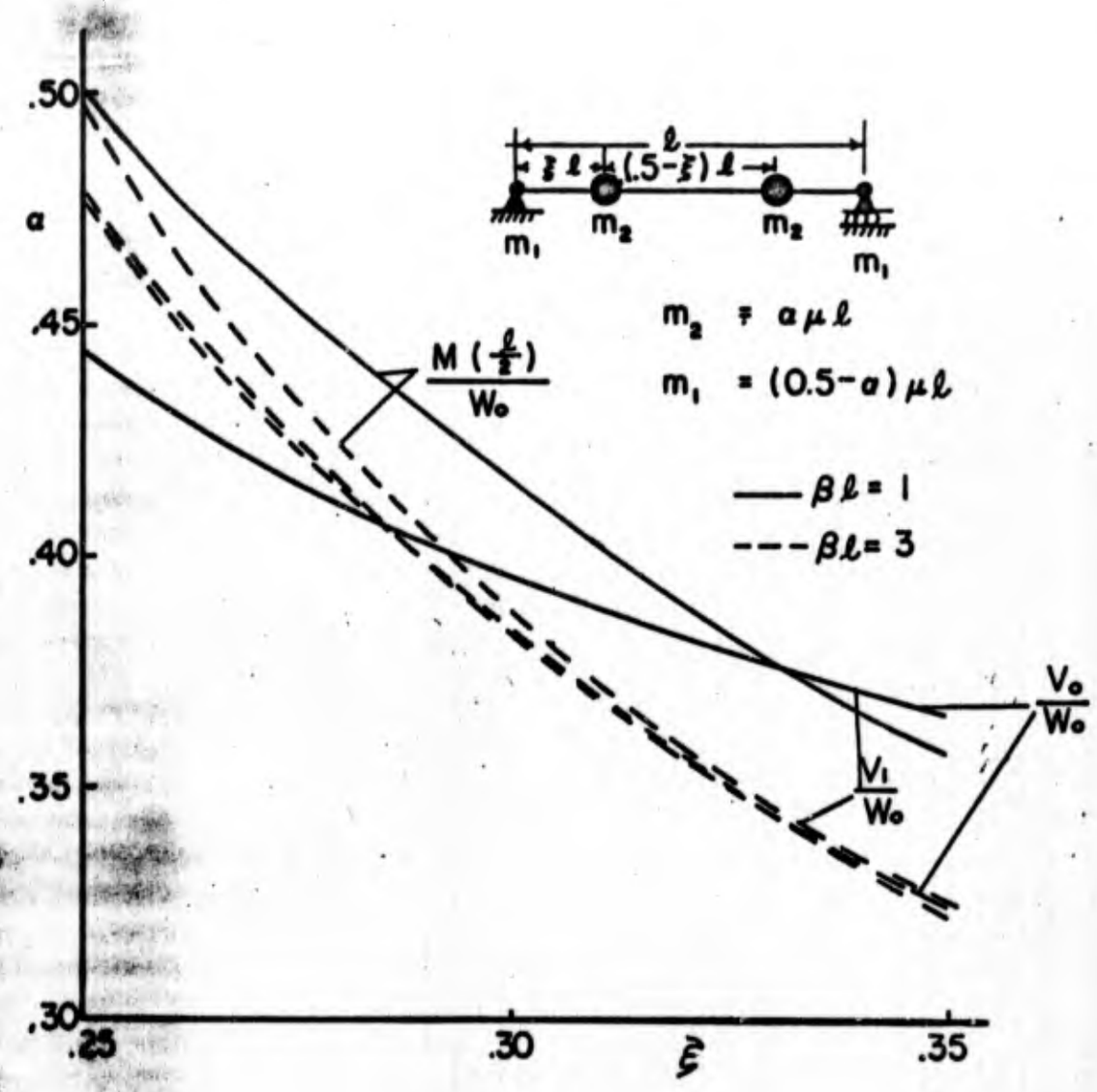

FIG. A-1 OPTIMIZING CONDITION FOR HINGED-HINGED BEAM

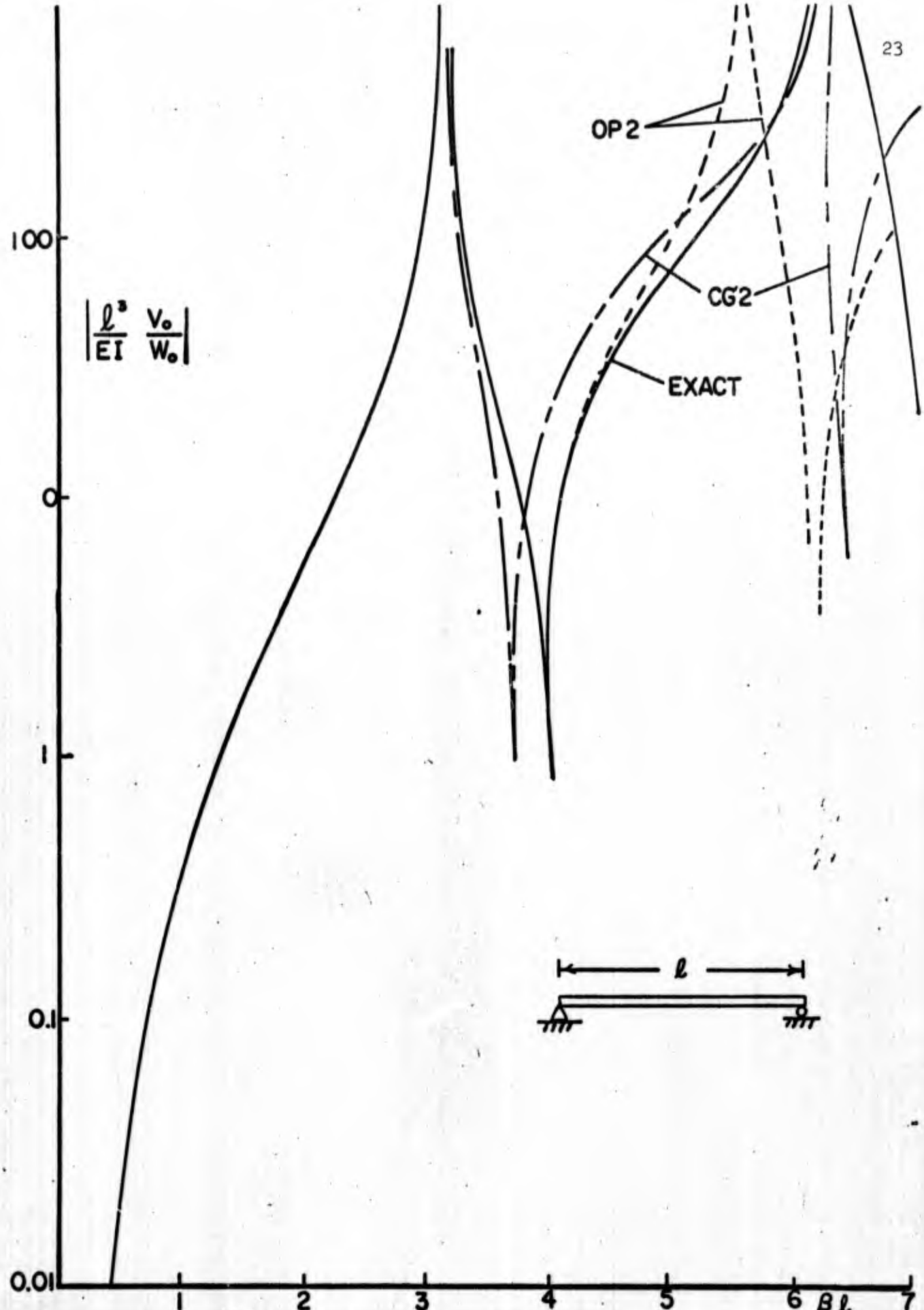

FIG. A-2 $\frac{V_o}{W_o}$ VS, $\beta\ell$, HINGED-HINGED BEAMS

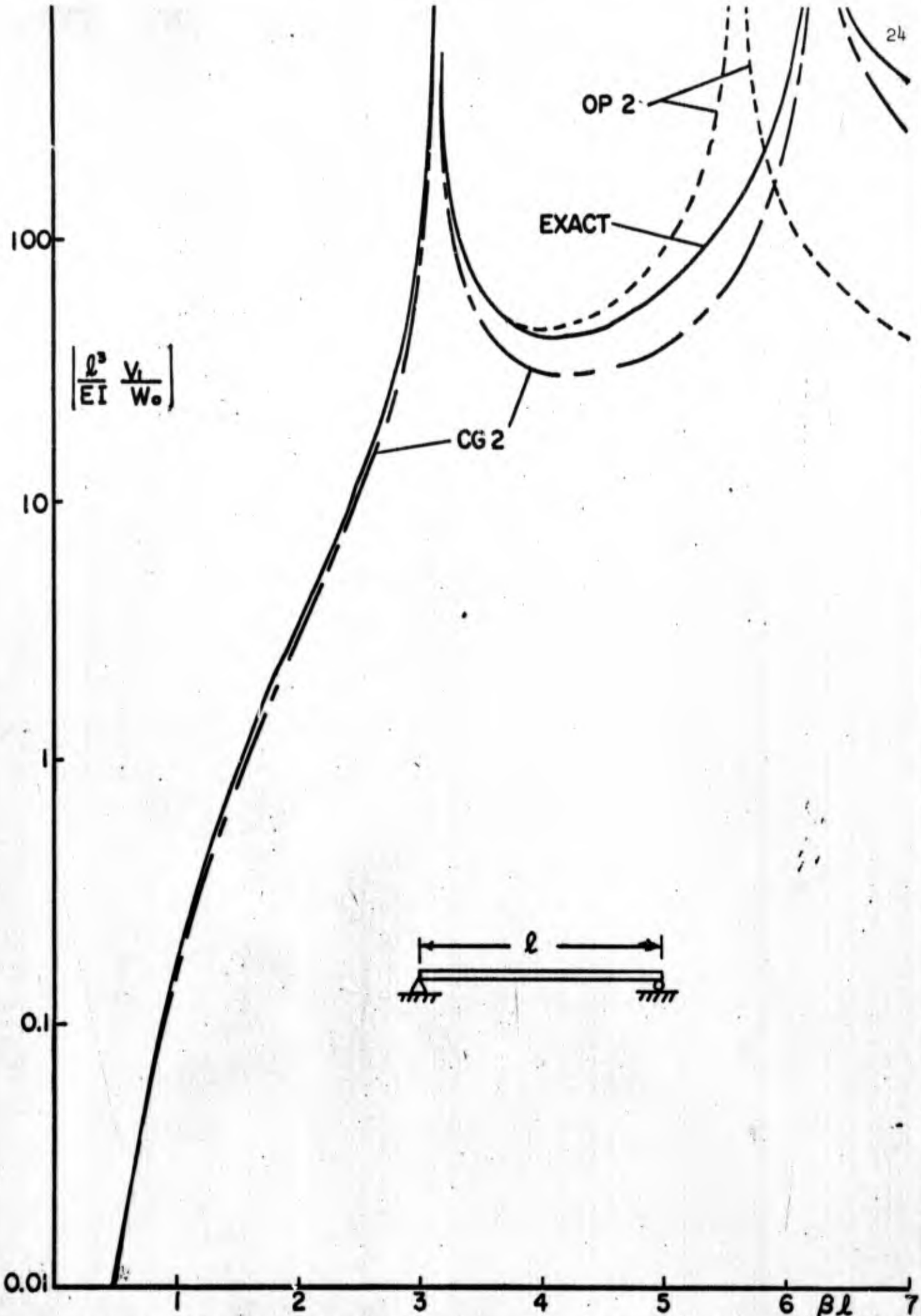

FIG. A-3 $\frac{V_1}{W_o}$ VS, $\beta\ell$, HINGED - HINGED BEAMS

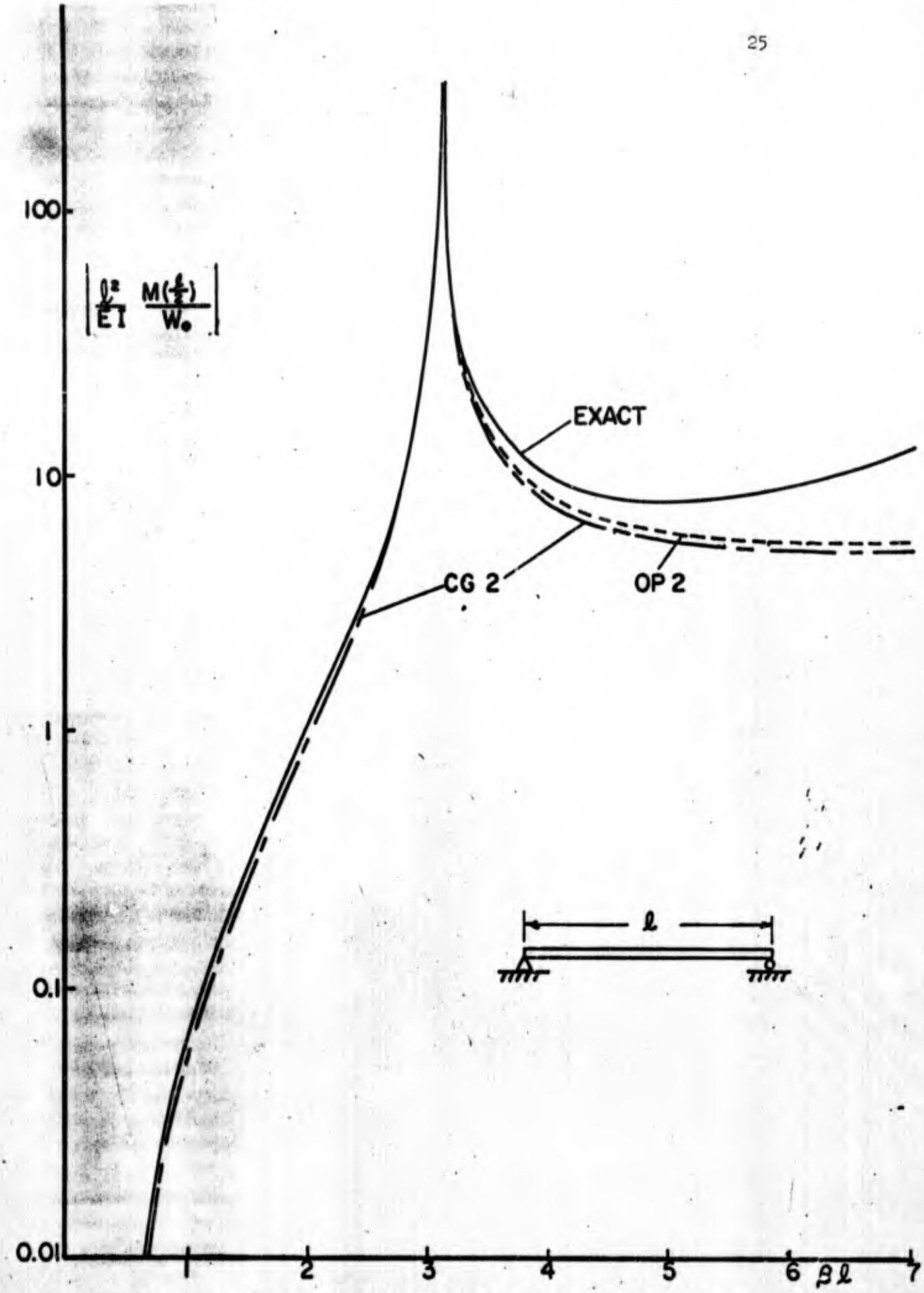

FIG. A-4 $M(\frac{l}{2})/W_o$ VS. βl, HINGED-HINGED BEAMS

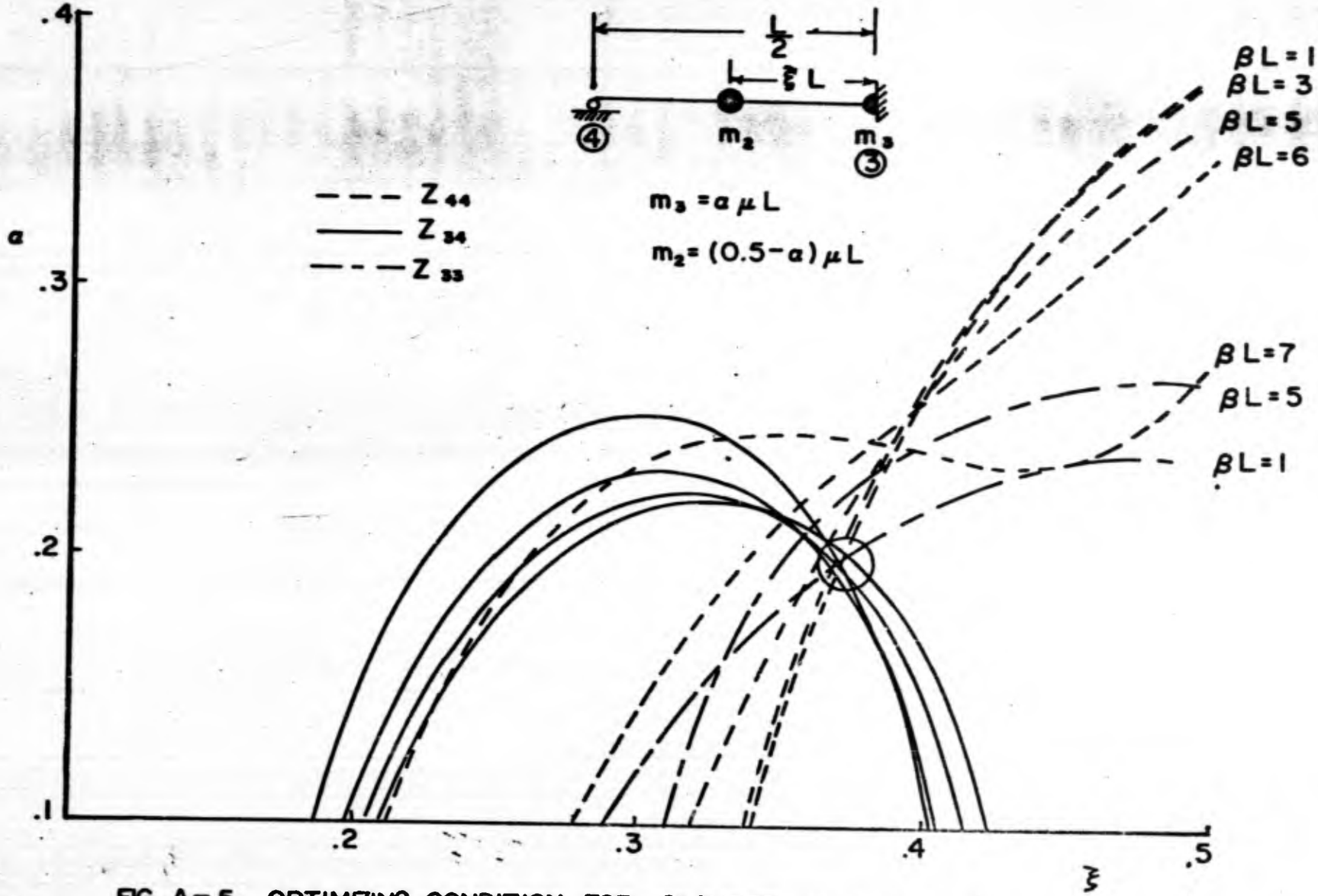

FIG. A-5 OPTIMIZING CONDITION FOR CLAMPED-PROPPED BEAM

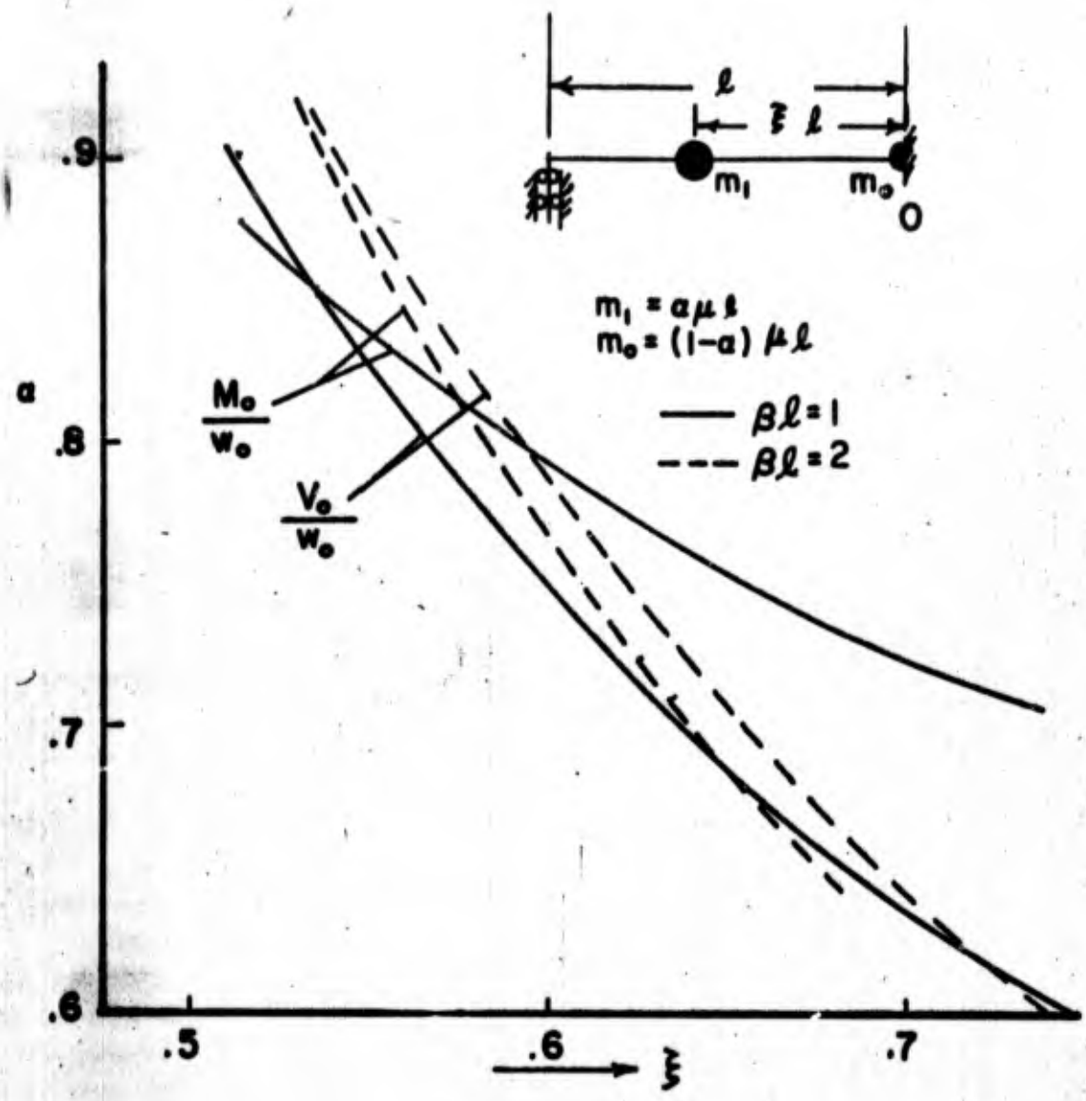

FIG. A-6 OPTIMIZING CONDITION FOR CLAMPED-GUIDED BEAM

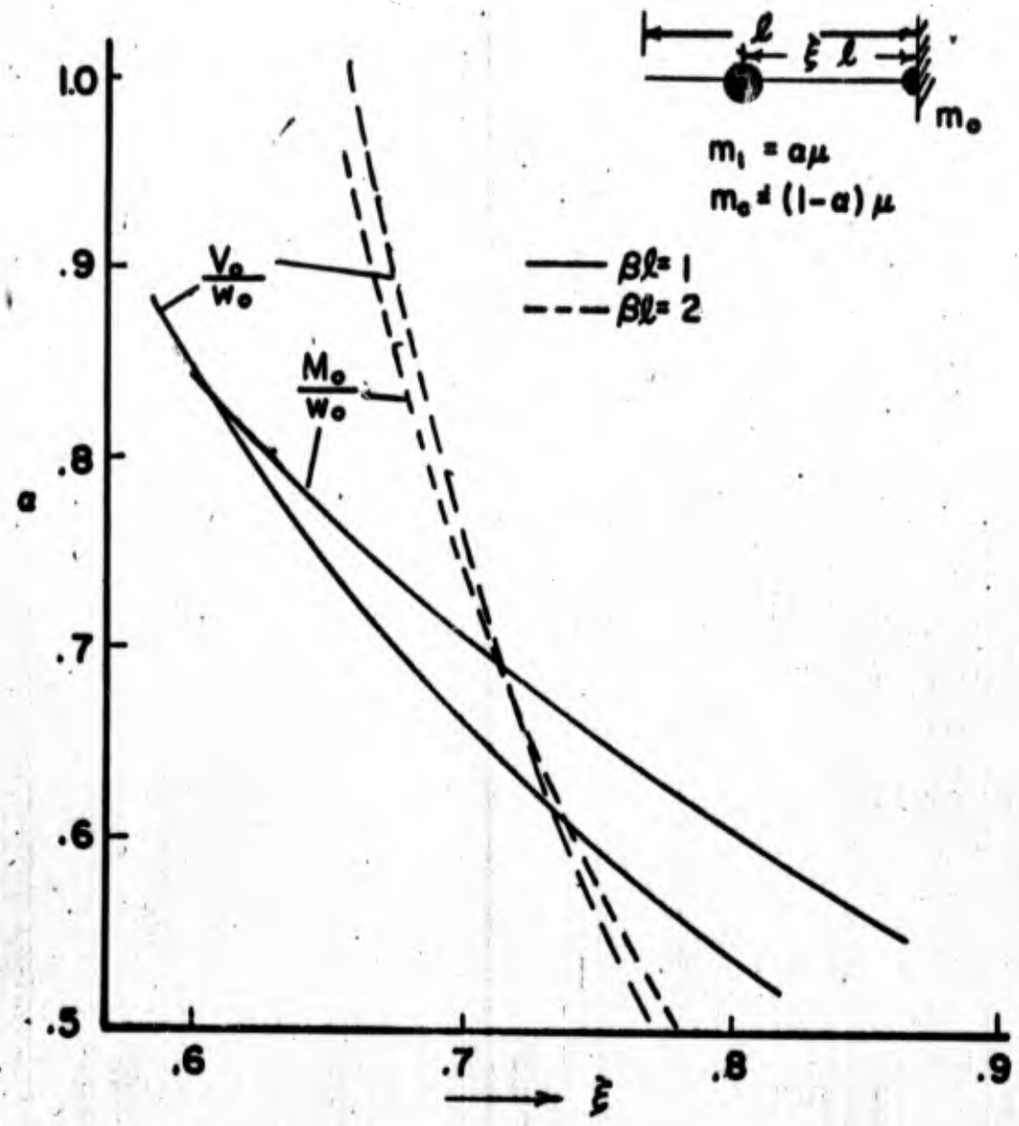

FIG. A-7 OPTIMIZING CONDITION FOR CLAMPED-FREE BEAM

Appendix B

Bar Models Using Mobility

The development of bar models using the mobility is discussed in detail elsewhere.[2,3] Point mobility at the end of a free-free uniform bar may be expressed in the following alternate ways:

$$M = -\frac{j}{A\rho a}\left[\frac{\text{Cos}p}{\text{Sin}p}\right] \tag{B-1}$$

where $p = \frac{\omega \ell}{a}$, A is cross-sectional area, ρ is mass density, ℓ is the bar length, and a is the speed of sound in the material.

In terms of normal modes, the general form of the series is

$$M_{11} = j\omega\left[-\frac{1}{\gamma_o \omega^2} + \sum_{n=1}^{\infty} \frac{1}{\gamma_{ii,n}(\omega_n^2 - \omega^2)}\right] \tag{B-2}$$

For the bar, the series is

$$M_{11} = \frac{jp}{A\rho a}\left[-\frac{1}{p^2} + \sum_{n=1}^{\infty} \frac{2}{p_n^{\,2} - p^2}\right]$$

The power series is

$$M_{11} = j\omega\left[-\frac{a_o}{\omega^2} + a_1 + a_2\omega^2 + a_4\omega^4 + \ldots\right] \tag{B-3}$$

Also, in terms of natural frequencies ω_n and antiresonant frequencies q_n

$$M_{11} = -\frac{j\omega}{\gamma_o \omega^2}\left[\left(1-\frac{\omega^2}{q_1^2}\right)\left(1-\frac{\omega^2}{q_2^2}\right)\ldots\left(1-\frac{\omega^2}{q_n^2}\right) \Big/ \left(1-\frac{\omega^2}{\omega_1^2}\right)\left(1-\frac{\omega^2}{\omega_2^2}\right)\ldots\left(1-\frac{\omega^2}{\omega_n^2}\right)\right] \tag{B-4}$$

Models were derived to match various quantities. The models carried two to four masses as shown in Fig. B-1. The models are designated by two letters and a number. The number indicates the number of masses in the model. A CG indicates the usual center of gravity positioning. Some of the models developed and the quantities matched are summarized in Table B-I. For example, for Model AR4 the total mass, or γ_0; two natural or resonant frequencies, p_1 and p_2; and one antiresonant frequency, q_2, were matched using a symmetrical model. The values of $\gamma_{11,n}$ are modal effective masses, as in (B-2) associated with point mobility for the first mode. Effective masses for transfer mobility between the two ends of the rod are indicated as $\gamma_{13,n}$.

Some combinations of models were considered as indicated in Fig. B-1. The basis for connecting two segments of uniform bar or two models is indicated in Figure B-2. In Table B-II, some of the parameters of the derived models are compared with those of the uniform bar. Other results are given in Ref. 3 for combinations of models. Mobility curves are also shown, which dramatically demonstrate the advantages of the various derived models in certain frequency ranges.

In Table B-III, the coefficients of the power series expansion (B-3) are compared. No models were derived specifically by matching terms in the power series except BP-2. The success of this model in predicting low frequency transient response led to the use of the power series approach and the α-ξ plots for beams reported in the first part of the report.

Transient Response

The input to the end of the bar was a half-sine pulse, or

$$F_1(t) = f_1 \operatorname{Sin} \frac{\pi t}{\tau} \qquad 0 \leq t \leq \tau$$
$$= 0 \qquad t \leq \tau \qquad \text{(B-5)}$$

Impulses of two different durations were considered. For one $\frac{\pi}{\tau} = 0.1333$ a/ℓ and for the other $\frac{\pi}{\tau} = .7833$ a/ℓ. Note that the first bar natural frequency occurs at $\omega_1 = \frac{\pi a}{\ell}$. In Figs. B-3(a) and B-3(b) the response to the lowest frequency input is compared for various models. The exact normal mode series converges rather slowly, so the sum of 100 terms is compared with the sum of 20 terms. The response of CG7 was almost identical to the exact solution. The most important result is that the accuracy of the response of the models is directly related to the accuracy of the low frequency mobility, as indicated in Table B-III. Also, it is significant that the derived two or three mass models were as adequuate as the six or seven mass CG models.

Table B-I. Model Designations with Quantities Matched and Resulting Values of Masses and Spring Constants.

Desig.	m_1/m_b	m_2/m_b	K_1	K_2	Quantities Matched
CG2	0.5000	0.5000	1.0000	none	γ_o, sym.
OP2	0.3333	0.6667	2.1932	none	$\gamma_{11,1}$, γ_o, p_1
BP2	0.5000	0.5000	0.7500	none	γ_o, a_1, sym.
CG3	0.2500	0.5000	2.0000	none	γ_o, sym.
OP3	0.2500	0.5000	2.4674	none	γ_o, p_1, $\gamma_{11,1}$, sym.
AP3	0.2143	0.5714	2.1149	none	γ_o, p_1, q_1, sym.
CG4	0.1667	0.3333	3.0000	3.0000	γ_o, sym.
AP4	0.1066	0.3934	3.3112	2.7124	γ_o, p_1, p_2, q_1, sym.
AR4	0.1597	0.3403	4.2909	2.9249	γ_o, p_1, p_2, q_2, sym.

Table B-II. Natural Frequencies p_n and Modal Effective Masses $\gamma_{11,n}$ and $\gamma_{13,n}$ for Various Models

Desig.	First Mode			Second Mode			Third Mode		
	p_1	$\gamma_{11,1}/m_b$	$\gamma_{13,1}/m_b$	p_2	$\gamma_{11,2}/m_b$	$\gamma_{13,2}/m_b$	p_3	$\gamma_{11,3}/m_b$	$\gamma_{13,3}/m_b$
CG2	0.6366	1.0000	-1.0000	none	....	....	none	....	....
OP2	1.0000	0.5000	-1.0000	none	....	....	none	....	....
BP2	0.5713	1.0000	-1.0000	none	....	....	none	....	....
CG3	0.9003	0.5000	-0.5000	0.6366	1.0000	1.0000	none	....	....
OP3	1.0000	1.5000	-0.5000	0.7071	1.0000	1.0000	none	....	....
AP3	1.0000	0.4285	-0.4285	0.6614	0.7500	0.7500	none	....	....
CG4	0.9549	0.5000	-0.5000	0.8270	0.5000	+0.5000	0.6366	1.0000	-1.0000
AP4	1.0000	0.5794	-0.5794	1.0000	0.2710	0.2710	0.6990	0.3373	-0.3373
AR4	1.0000	0.5918	-0.5918	1.0000	0.4693	0.4693	0.7258	0.6938	-0.6938
Uniform	1.0000	0.5000	-0.5000	1.0000	0.5000	0.5000	1.0000	0.5000	-0.5000

Table B-III(a). Natural Frequencies p_n and Effective Masses $\gamma_{11,n}$ and $\gamma_{13,n}$ for Various Models for n = 1, 2, 3.

No. of Masses	System	First Mode		Second Mode		Third Mode	
		p_1	$\gamma_{11,1}/m_b$	p_2	$\gamma_{11,2}/m_b$	p_3	$\gamma_{11,3}/m_b$
4	OP3-OP2	1.1174	0.4815	1.0000	0.5000	0.9020	0.3421
5	CG5	0.9745	0.5000	0.8533	0.5000	0.7842	0.5000
5	OP3-OP3	1.0824	0.5000	1.0000	0.5000	0.8710	0.5000
5	AP3-AP3	1.0000	0.5357	1.0000	0.4286	0.8165	0.3571
7	CG7	0.9886	0.5000	0.9549	0.5000	0.9003	0.5000
7	AP3-AP3-AP3	1.0158	0.5129	0.9771	0.5930	1.0000	0.4286
7	AP4-AP4	1.0000	0.5360	1.0000	0.5794	0.9237	0.9094
7	AR4-AR4	1.0978	0.4887	1.0000	0.5918	1.0000	0.9227

Table B-III(b). Natural Frequencies p_n and Effective Masses $\gamma_{11,n}$ and $\gamma_{13,n}$ for Various Models for n = 1, 2, 3.

No. of Masses	System	Fourth Mode		Fifth Mode		Sixth Mode	
		p_4	$\gamma_{11,4}/m_b$	p_5	$\gamma_{11,5}/m_b$	p_6	$\gamma_{11,6}/m_b$
4	OP3-OP2	....	....	....	....	....	....
5	CG5	0.6366	1.0000	....	....	....	....
5	OP3-OP3	0.7072	1.0000	....	....	....	....
5	AP3-AP3	0.6614	0.7500	....	....	....	....
7	CG7	0.8270	0.5000	0.7379	0.5000	0.6366	1.0000
7	AP3-AP3-AP3	0.8635	0.3355	0.7673	0.3681	0.6614	0.7500
7	AP4-AP4	1.0000	0.2710	0.8222	0.1559	0.6990	0.3373
7	AR4-AR4	1.0000	0.4692	0.8455	0.3193	4.3551	0.6938

SIMPLE MODELS

TWO MASS

THREE MASS

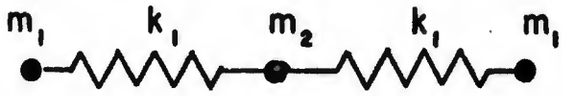

FOUR MASS

COMBINATIONS

OP3 − OP2

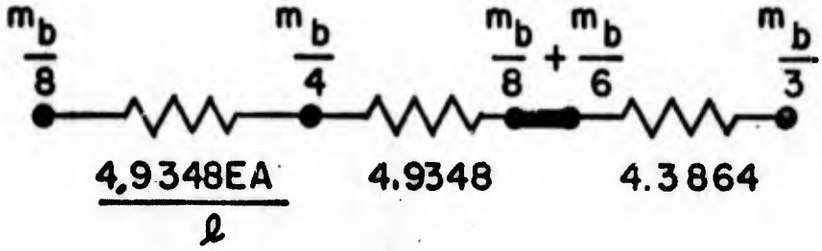

OP3 − OP3

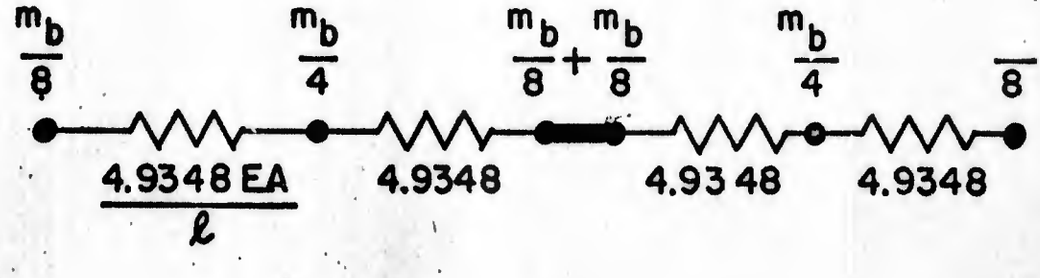

FIG. B-1

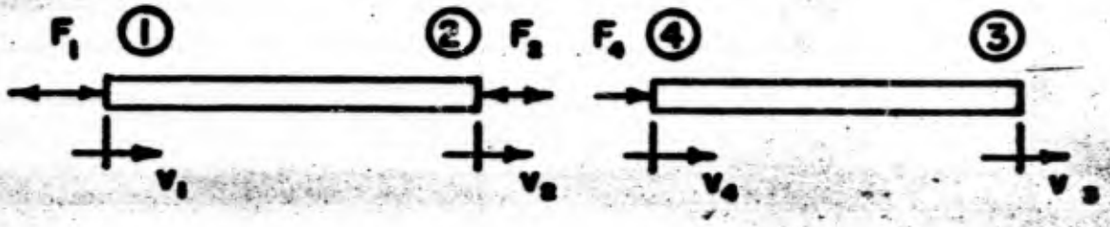

IN COMBINATION, $V_2 = V_4$

$F_2 = -F_4$

FIG. B-2

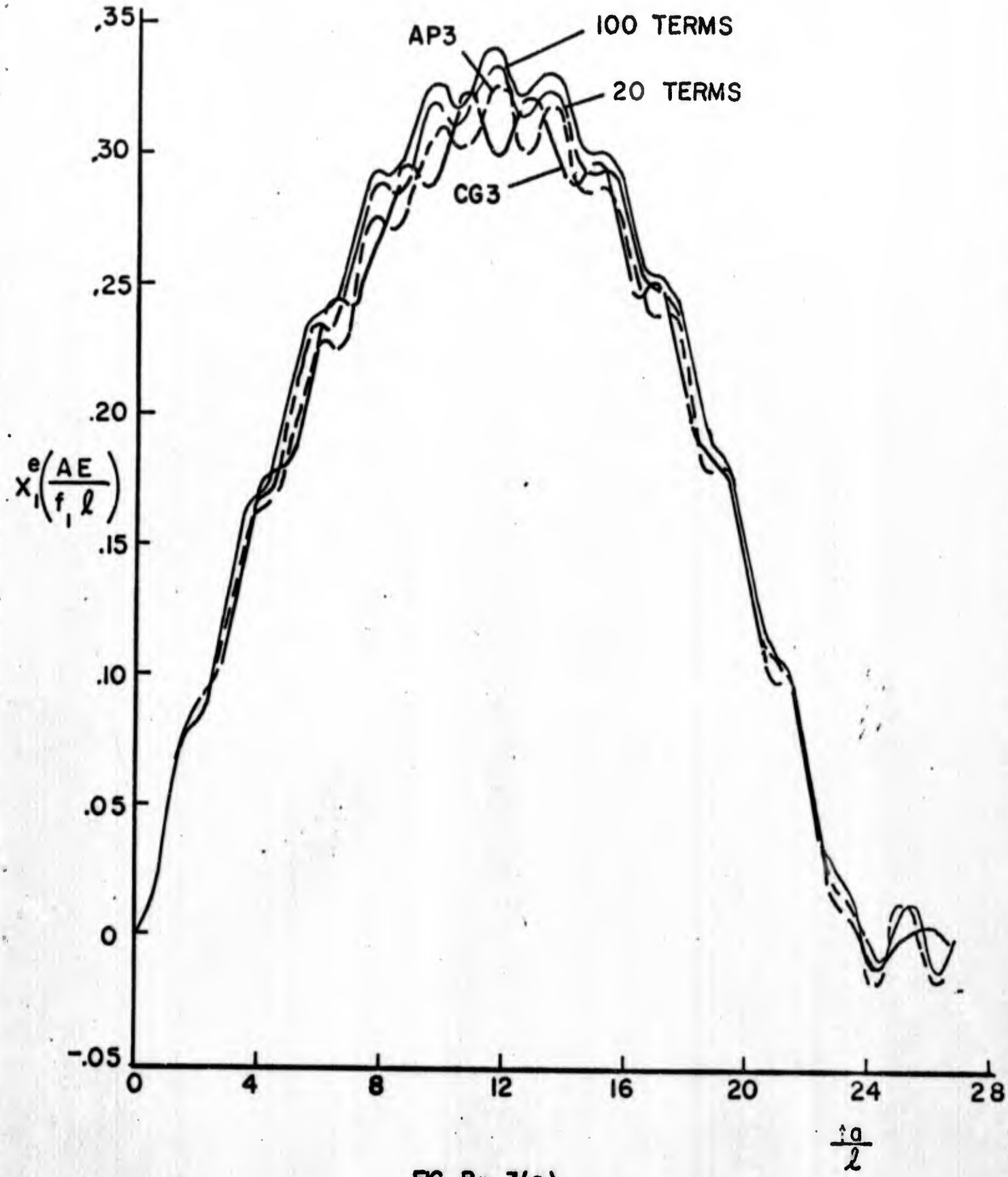
AP3
100 TERMS
20 TERMS
CG3
.35
.30
.25
.20
.15
.10
.05
0
-.05
$X_1^e\left(\frac{AE}{f_1 \ell}\right)$
0
4
8
12
16
20
24
28
$\frac{\pm a}{\ell}$

FIG, B- 3(a)

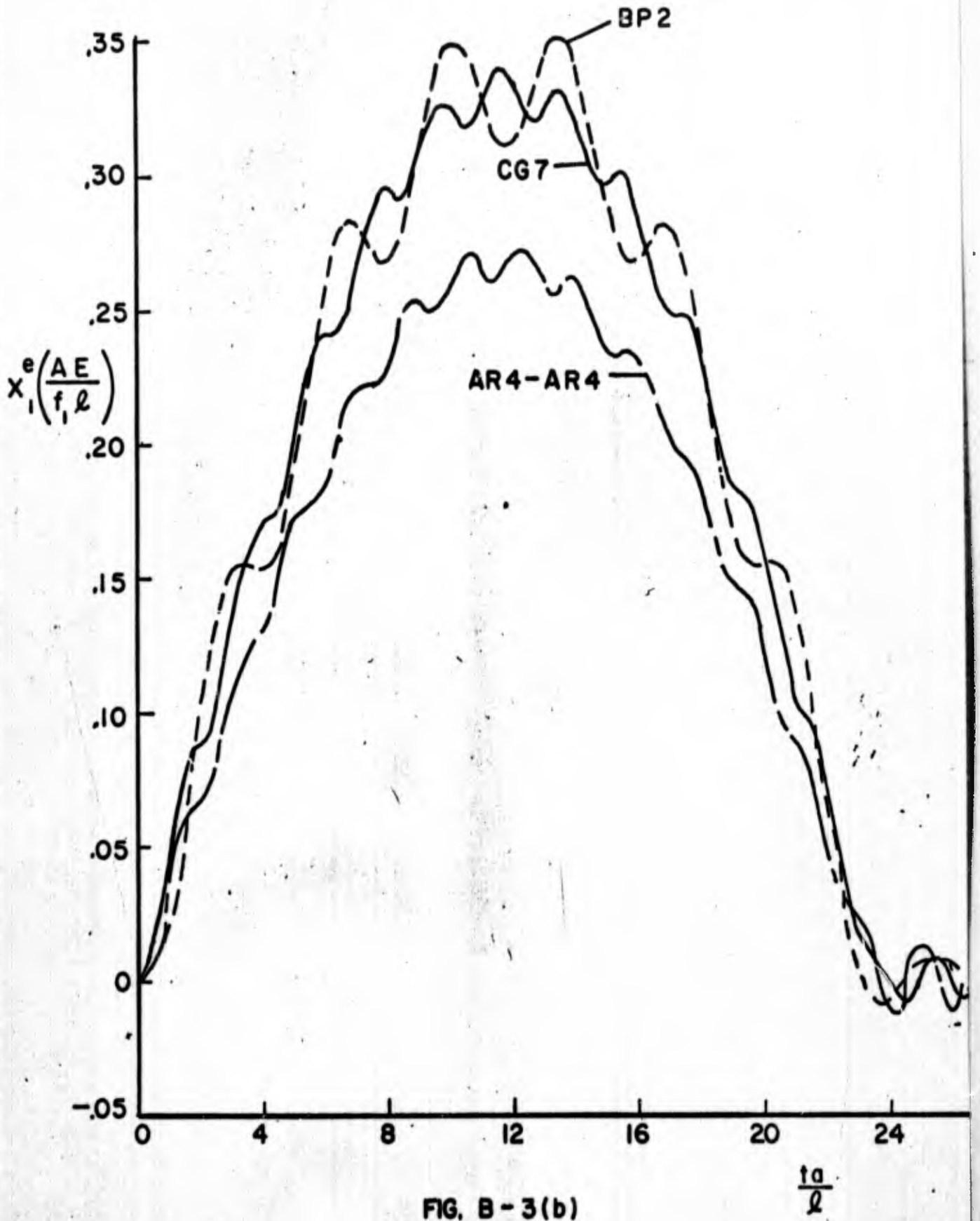
BP2
CG7
AR4-AR4
.35
.30
.25
.20
.15
.10
.05
0
-.05
$X_1^e\left(\frac{AE}{f_1 \ell}\right)$
0
4
8
12
16
20
24
$\frac{ta}{\ell}$

FIG. B-3(b)

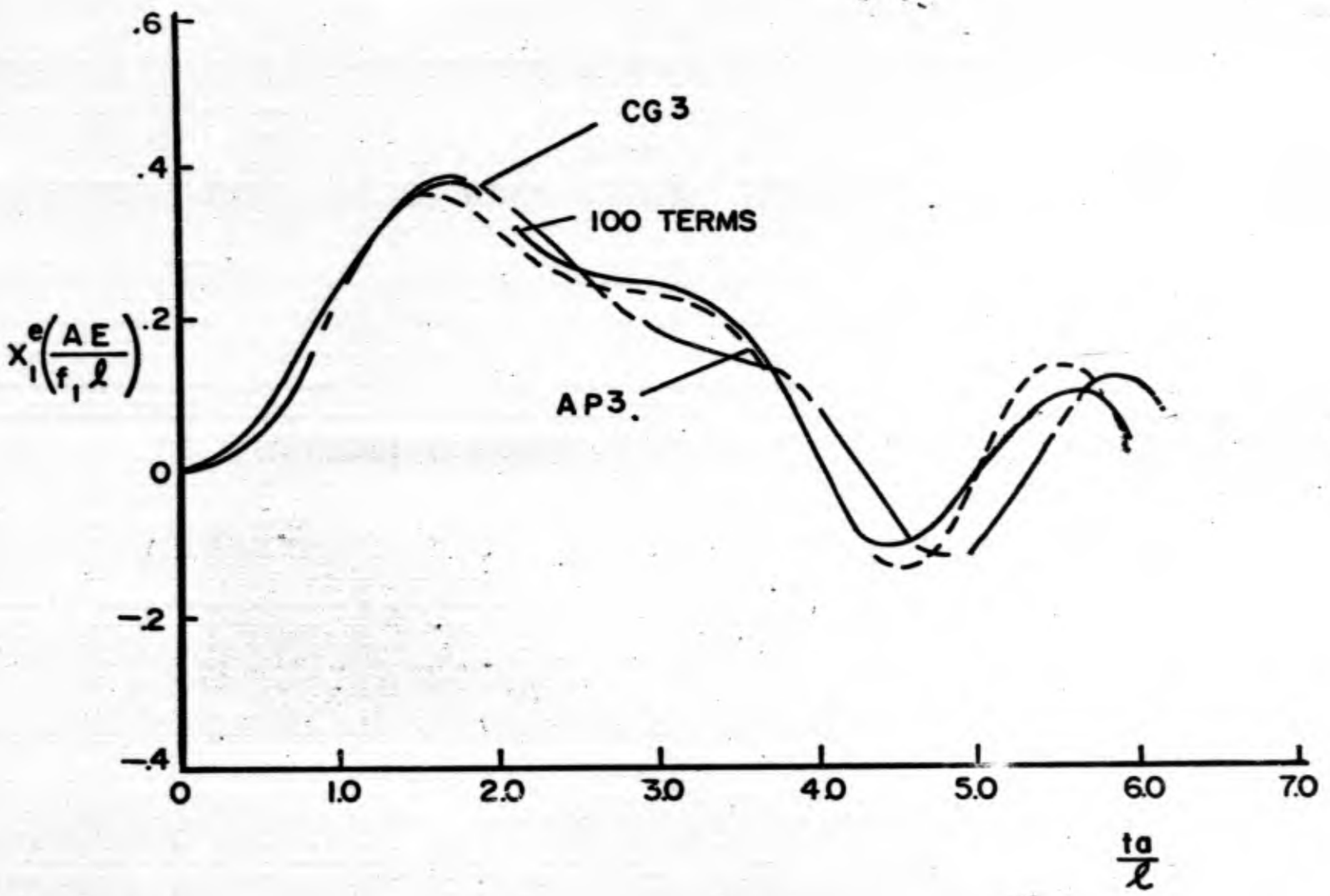
.6
.4
.2
0
-.2
-.4
$X_1^e\left(\frac{AE}{f_1 \ell}\right)$
CG 3
100 TERMS
AP3.
0
1.0
2.0
3.0
4.0
5.0
6.0
7.0
$\frac{ta}{\ell}$

FIG. B-4(a)

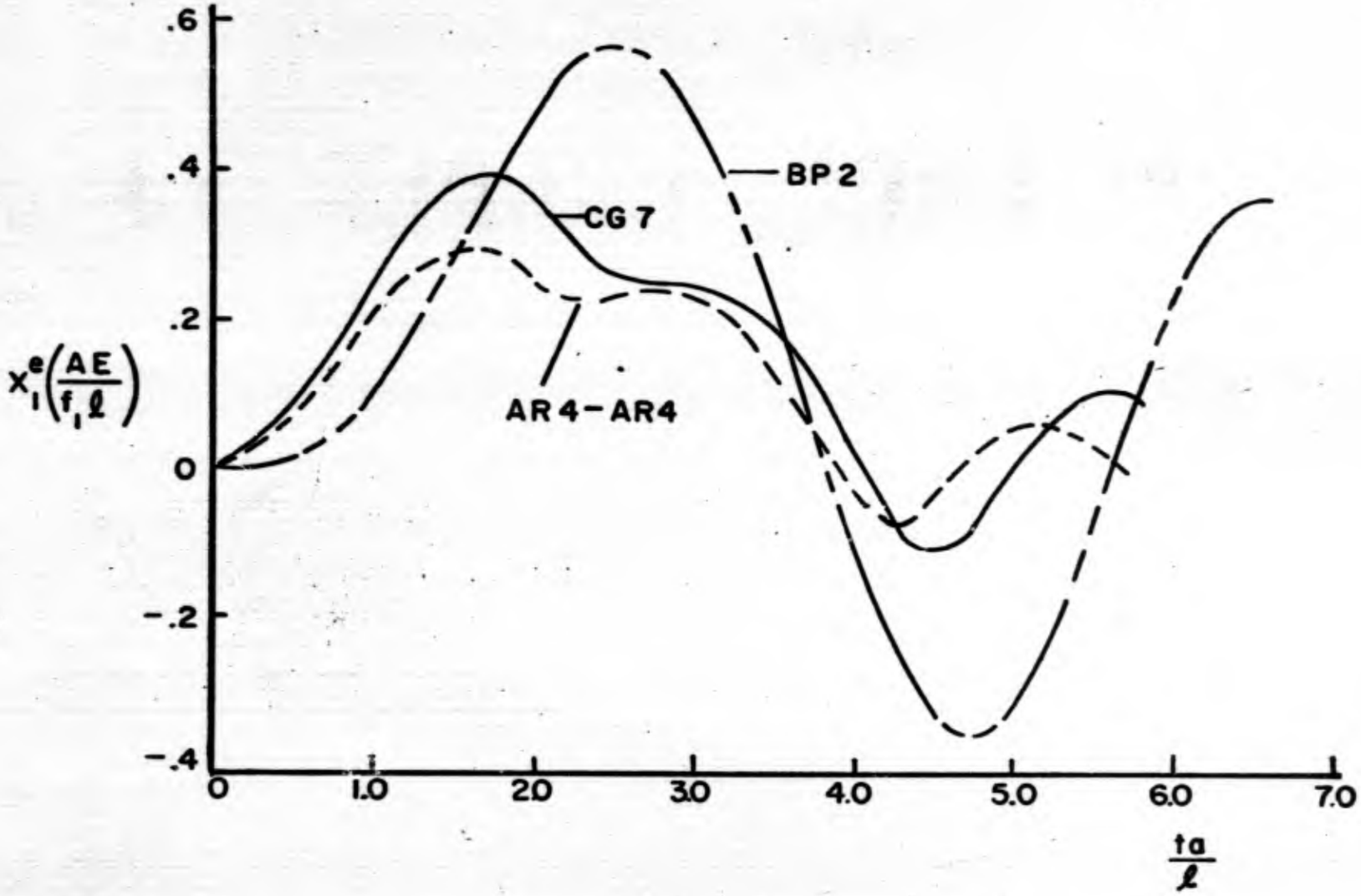
.6
.4
.2
0
-.2
-.4
$x_1^e\left(\frac{AE}{f_1 \ell}\right)$
BP 2
CG 7
AR 4 – AR 4
0
1.0
2.0
3.0
4.0
5.0
6.0
7.0
$\frac{ta}{\ell}$

FIG. B – 4(b)

Appendix C

Optimum Models Based on Shock Effective Mass Approach

Uniform Beam

As an end result, it is desired that improved models more adequately represent the response of structures to ground shock input. It is well known that modal shock effective masses and natural frequencies are important parameters, and in fact some design methods assume knowledge of these parameters for shock analysis.[6] For ground shock in which variation of ground velocity is a step function of magnitude v_o, the relative elastic displacement of the beam is

$$y(x,t) = - \sum \phi_n(x) \frac{\gamma_n v_o}{\omega_n} \mathrm{Sin}\omega_n t \qquad (C1)$$

The $\phi_n(x)$ is the mode shape and γ_n is the modal participation factor:

$$\gamma_n = \frac{\int_o^\ell \mu \, \phi_n(x)dx}{\int_o^\ell \mu \, \phi_n^2(x)dx} \qquad (C2)$$

The natural frequencies ω_n are related to the beam stiffness EI and beam mass per unit length μ by

$$\omega_n^2 = \frac{\beta_n^4 \, EI}{\mu} \qquad (C3)$$

The shear at the base is

$$V(x,t) = EI \, y'''(x,t) = - \sum_n \frac{EI\gamma_n v_o}{\omega_n} \phi_n'''(\ell)\mathrm{Sin}\omega_n t \qquad (C4)$$

The general form of (C4) is that of force is equal to mass times accelerations, or

$$V(x,t) = \sum_n \ (\text{mass})_n \ (v_o \omega_n \text{Sin}\omega_n t) \qquad (C5)$$

For bending moment, the equation is

$$B(x,t) = \sum_n \ (\text{mass} \times \text{arm})_n (v_o \omega_n \text{Sin}\omega_n t) \qquad (C6)$$

At the base of a clamped-free beam:

$$V(0,t) = - \sum \frac{4\alpha_n^2 (\mu\ell)^2}{M_n (\beta_n \ell)^2} \ v_o \omega_n \text{Sin}\omega_n t = - \sum V_{on} \text{Sin}\omega_n t \qquad (C7)$$

$$B(0,t) = \sum \frac{4\ell(\mu\ell)^2 \alpha_n}{M_n (\beta_n \ell)^3} \ v_o \omega_n \text{Sin}\omega_n t = \sum B_{on} \text{Sin}\omega_n t \qquad (C8)$$

The values of α_n, β_n, and $\phi_n(x)$ are given in tables by Young and Felgar.[8]

For a hinged-hinged beam, the shear at the support and the moment at the center point are

$$V(0,t) = - \sum \frac{4\mu\ell}{n^2\pi^2} \ v_o \omega_n \text{Sin}\omega_n t = - \sum V_{on} \text{Sin}\omega_n t \qquad (C9)$$

$$B(\tfrac{\ell}{2},t) = \sum \frac{4\mu\ell^3}{n^3\pi^3} \ \text{Sin} \frac{n\pi}{2} \ v_o \omega_n \text{Sin}\omega_n t = \sum B_{cn} \text{Sin}\omega_n t \qquad (C10)$$

Lumped Mass Beam

For a weightless beam carrying lumped masses, m_i, the dynamic force F_{in}, at the i^{th} mass for the n^{th} mode, associated with a step velocity base motion is

$$F_{in} = \frac{P_n m_i \phi_{in}}{M_n} \ v_o \omega_n \text{Sin}\omega_n t \qquad (C11)$$

where $$M_n = \sum_i m_i \phi_{in}^2 \tag{C12}$$

and $$P_n = \sum_i m_i \phi_{in} \tag{C13}$$

For a cantilever beam with one mass m_1 a distance h_1 from the base (Fig. C-1) the shear and bending moment for the n^{th} mode is

$$V(0,t) = - m_1 v_o \omega_n \mathrm{Sin}\omega_n t \tag{C14}$$

$$B(0,t) = m_1 h_1 v_o \omega_n \mathrm{Sin}\omega_n t \tag{C15}$$

For the cantilever with two masses (Fig. C-1)

$$V(0,t)_n = - \frac{P_n}{M_n} v_o \omega_n \mathrm{Sin}\omega_n t (m_1 \phi_{1n} + m_2 \phi_{2n}) \tag{C16}$$

$$B(0,t) = \frac{P_n}{M_n} v_o \omega_n \mathrm{Sin}\omega_n t (m_1 \phi_{1n} h_1 + h_2 m_2 \phi_{2n}) \tag{C17}$$

For the hinged-hinged beam with three masses (Fig. C-2):

$$V(0,t) = - \left(\sum_n F_{1n} + \frac{1}{2} F_{2n} \right) \tag{C19}$$

$$B(\tfrac{\ell}{2},t) = \sum_n F_{1n} h_1 + \frac{F_{2n}\ell}{4} \tag{C20}$$

Development of Lumped-Mass Models

A lumped-mass model of a cantilever beam is assumed to carry a mass m_1 a distance h_1 from the support on a beam having a fictitious bending stiffness E'I'. To match (C14) with the first term in (C7):

$$\frac{V_{o1}}{v_o \omega_1} = .6131\, \mu\ell = m_1 \tag{C21}$$

For bending moment, from (C15) and (C8)

$$\frac{B_{o1}}{v_o \omega_1} = .4454\ \mu\ell^2 = m_1 h_1 \qquad (C22)$$

From (C21) and (C22)

$$m_1 = .6131\ \mu\ell \quad \text{and} \quad h_1 = .7265\ \ell \qquad (C23)$$

The frequency for the lumped mass system is

$$\omega_1^2 = \frac{3E'I'}{m_1 h_1^3} \qquad (C24)$$

To have ω_1 also the same as for the uniform system, one might choose E'I' = .9686 EI. The idea of using a value of EI different from that of the original beam has not been pursued in general.

The first two lines in Table C-I are associated with this example. In the first line E'I' = EI and in the second line, the case where E'I' = .9686 EI is shown. In the bottom line are listed the values for the first two modes of a uniform beam.

For a two mass cantilever the positioning is already much more difficult. There are now four parameters available - magnitudes and positions of the two masses. The numbers matched are the value of base shear for first and second modes (C25) and (C26), the first mode moment factor (C27) and the first mode frequency (C28). These are expressed in terms of the modal amplitudes ϕ_{1n}. If $\phi_{11} = 1$ and $\phi_{12} = 1$, then ϕ_{21} and ϕ_{22} are two additional unknowns, bringing the total to six. Two additional equations are required involving the orthogonality of the modes (C29) and (C30).

$$\frac{m_1^2\phi_{11}^2 + m_1 m_2 \phi_{11}\phi_{21}}{m_1\phi_{11}^2 + m_2\phi_{21}^2} + \frac{m_1 m_2 \phi_{11}\phi_{21} + m_2^2\phi_{21}^2}{m_1\phi_{11}^2 + m_2\phi_{21}^2} = .6131\ \mu\ell \qquad (C25)$$

$$\frac{m_1^2\phi_{12}^2 + m_1 m_2 \phi_{12}\phi_{22}}{m_1\phi_{12}^2 + m_2\phi_{22}^2} + \frac{m_1 m_2 \phi_{12}\phi_{22} + m_2^2\phi_{22}^2}{m_1\phi_{12}^2 + m_2\phi_{22}^2} = .1883\ \mu\ell \qquad (C26)$$

$$\left(\frac{m_1\phi_{11}^2 + m_1 m_2 \phi_{11}\phi_{21}}{m_1\phi_{11}^2 + m_2\phi_{21}^2}\right)h_1 + \left(\frac{m_1 m_2 \phi_{11}\phi_{21} + m_2^2\phi_{21}^2}{m_1\phi_{11}^2 + m_2\phi_{21}^2}\right)h_2 = .4454\mu\ell^2 \qquad (C27)$$

$$\frac{m_1^2\phi_{11}^2\delta_{11} + 2m_1 m_2 \phi_{11}\phi_{21}\delta_{21} + m_2^2\phi_{21}^2\delta_{22}}{m_1\phi_{11}^2 + m_2\phi_{2i}^2} = \frac{1}{\omega_1^2} \qquad (C28)$$

$$m_1\phi_{11}\phi_{12} + m_2\phi_{21}\phi_{22} = 0 \qquad (C29)$$

$$m_1^2\phi_{11}\phi_{12}\delta_{11} + m_1 m_2 \phi_{12}\phi_{21}\delta_{21} + m_1 m_2 \phi_{11}\phi_{22}\delta_{12} + m_2^2\phi_{21}\phi_{22}\delta_{22} = 0 \qquad (C30)$$

The values of δ_{ij} are flexibilities and functions of h_1, h_2 and EI. Cubic powers of h_1 and h_2 are involved. To solve the six equations, the value of $\alpha = \frac{m_1}{m_2}$ is chosen. If (C25) and (C26) are added, the result is

$$m_1 + m_2 = .8014\ \mu\ell \qquad (C31)$$

Having chosen α, (C31) is solved for m_2. The value of ϕ_{21} is determined from (C25) and ϕ_{22} from (C29). Equation (C27) is then solved for h_2 in terms of h_1. The value of h_1 is then found from (C30). If the correct value of α is chosen, (C28) will be satisfied.

In Table C-I values are tabulated for α = 0.4, 1.0, and 1.5. For this large range of α, ω_1 varies only slightly. In Figure C-3(a), the values of h_1/ℓ and h_2/ℓ which satisfy the conditions imposed are shown versus α. A similar plot for B_{02} is shown in Figure C-3(b). The dotted line indicates the value of α to be chosen to make B_{02} agree with that for a uniform beam. Figures C-3(c) and C-3(d) show variation of ω_1 and ω_2 with α.

α	$\frac{E'I'}{EI}$	$\frac{m_1}{\mu\ell}$	$\frac{m_2}{\mu\ell}$	$\frac{h_1}{\ell}$	$\frac{h_2}{\ell}$	FIRST MODE			SECOND MODE		
						ω_1	$\frac{V_{on}}{v_o\omega_1\mu\ell}$	$\frac{B_{on}}{v_o\omega_1\mu\ell^2}$	ω_2	$\frac{V_{on}}{v_o\omega_2\mu\ell}$	$\frac{B_{on}}{v_o\omega_2\mu\ell^2}$
-	1.0000	.6131	-	.7265	-	4.3980	.6131	.4454	-	-	-
-	.9686	.6131	-	.7265	-	3.5160	.6131	.4454	-	-	-
-	1.0000	.5000	-	1.0000	-	2.4495	.5000	.5000	-	-	-
.4	1.0000	.2290	.5724	.9385	.4815	3.5147	.6131	.4454	17.07	.1883	.0451
1.0	1.0000	.4007	.4007	.8237	.3876	3.5216	.6131	.4454	23.70	.1883	.0399
1.5	1.0000	.4808	.3206	.7860	.3226	3.5281	.6131	.4454	30.37	.1883	.0360
.5	1.0000	.2500	.5000	1.0000	.5000	3.1562	.5637	.4522	16.26	.1863	.0478
UNIFORM BEAM						3.5160	.6131	.4454	22.03	.1883	.0394

TABLE C-I CLAMPED-FREE BEAM

α	$\frac{E'I'}{EI}$	$\frac{m_1}{\mu\ell}$	$\frac{m_2}{\mu\Pi}$	$\frac{h_1}{\ell}$	FIRST MODE			SECOND MODE		THIRD MODE	
					ω_1	$\frac{V_{on}}{v_o\omega_1\mu\ell}$	$\frac{B_{cn}}{v_o\omega_1\mu\ell^2}$	ω_2	ω_3	$\frac{V_{on}}{v_o\omega_3\mu\ell}$	$\frac{B_{cn}}{v_o\omega_3\mu\ell^2}$
-	1.0000	.8106	-	.5000	7.6953	.4053	.2026	-	-	-	-
-	1.6449	.8106	-	.5000	9.8696	.4053	.2026	-	-	-	-
-	1.0000	.5000	-	.5000	9.7980	.2500	.1250	-	-	-	-
-	1.0000	.4053	-	.2862	9.8696	.4053	.1160	31.44	-	-	-
-	1.0000	.4053	-	.3183	9.1988	.4053	.1290	33.26	-	-	-
-	1.0000	.3333	-	.3333	9.8590	.3333	.1111	38.18	-	-	-
.5	1.0000	.2252	.4503	.1694	9.2550	.4053	.1580	46.08	69.20	.0450	-.0073
.8	1.0000	.2771	.3464	.1742	9.8933	.4053	.1428	40.98	66.04	.0450	-.0079
1.0	1.0000	.3002	.3002	.1737	10.2562	.4053	.1353	39.43	65.78	.0450	-.0081
1.5	1.0000	.3377	.2252	.1690	11.0402	.4053	.1214	37.67	67.04	.0450	-.0080
1.0	1.0000	.2500	.2500	.2500	9.8078	.3657	.1293	49.57	61.43	.0093	-.0038
UNIFORM BEAM					9.8696	.4053	.1290	39.48	88.83	.0450	-.0048

TABLE C-II HINGED-HINGED BEAM

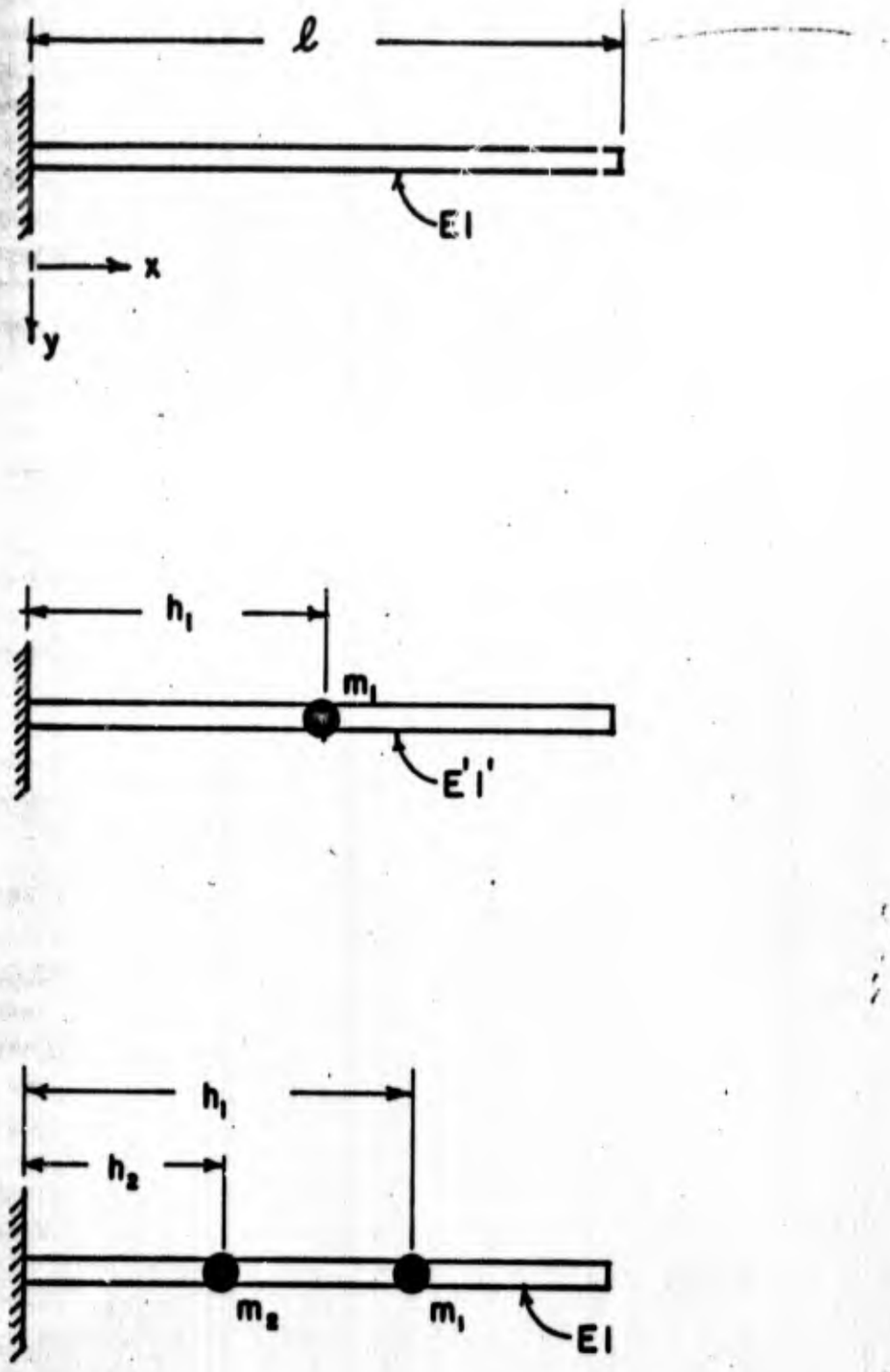

FIG. C-1 CLAMPED-FREE BEAMS

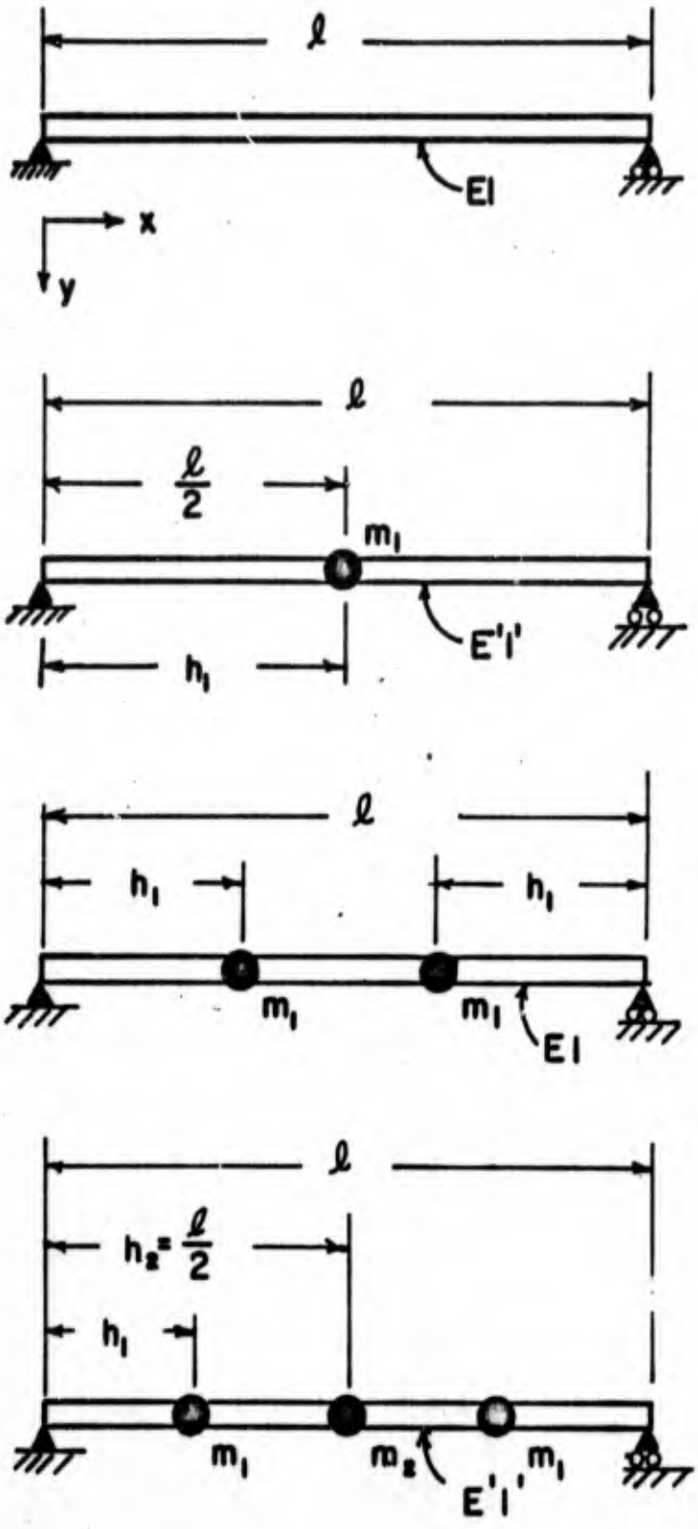

FIG. C-2 HINGED-HINGED BEAM

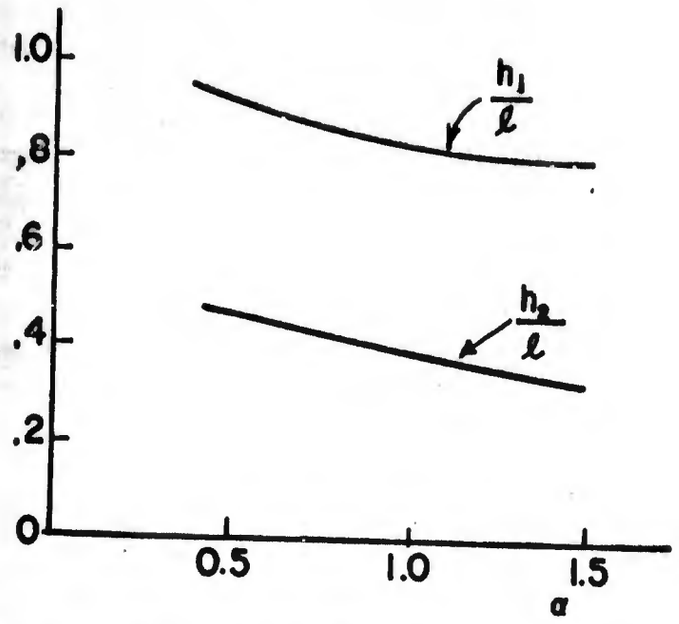

FIG. C-3(a) MASS POSITION VS. α

TWO MASS, CLAMPED-FREE BEAM

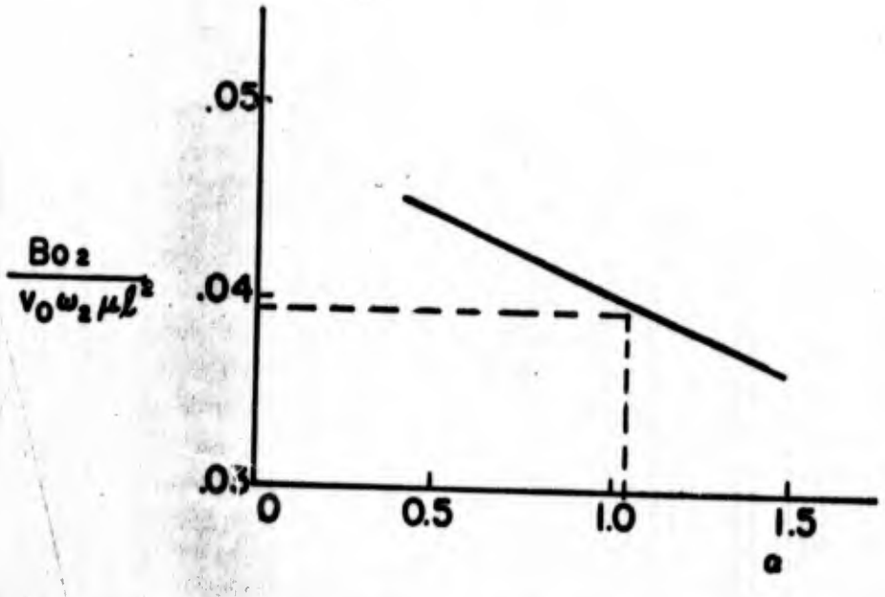

FIG. C-3(b) SECOND MODE BENDING MOMENT VS. α

TWO MASS, CLAMPED-FREE BEAM

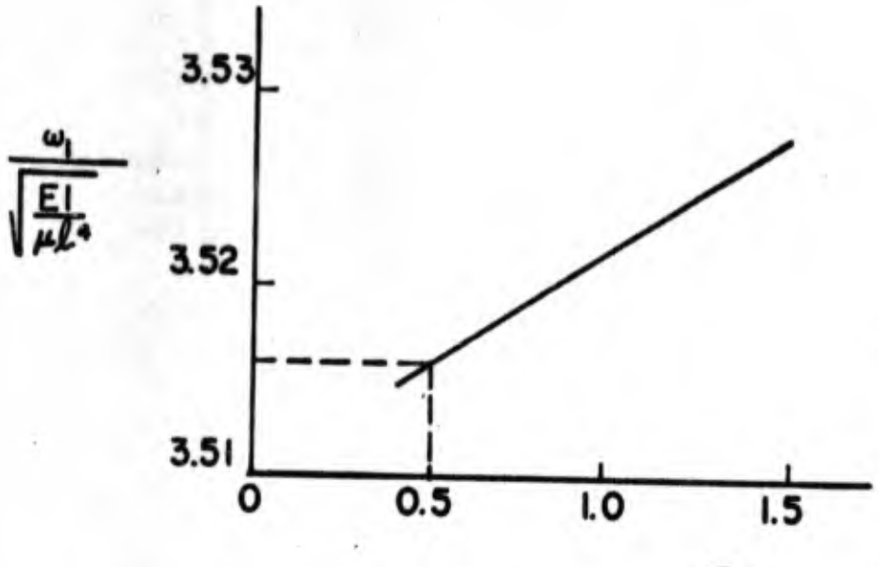

FIG. C-3(c) FIRST NATURAL FREQUENCY VS, α
TWO MASS, CLAMPED - FREE BEAM

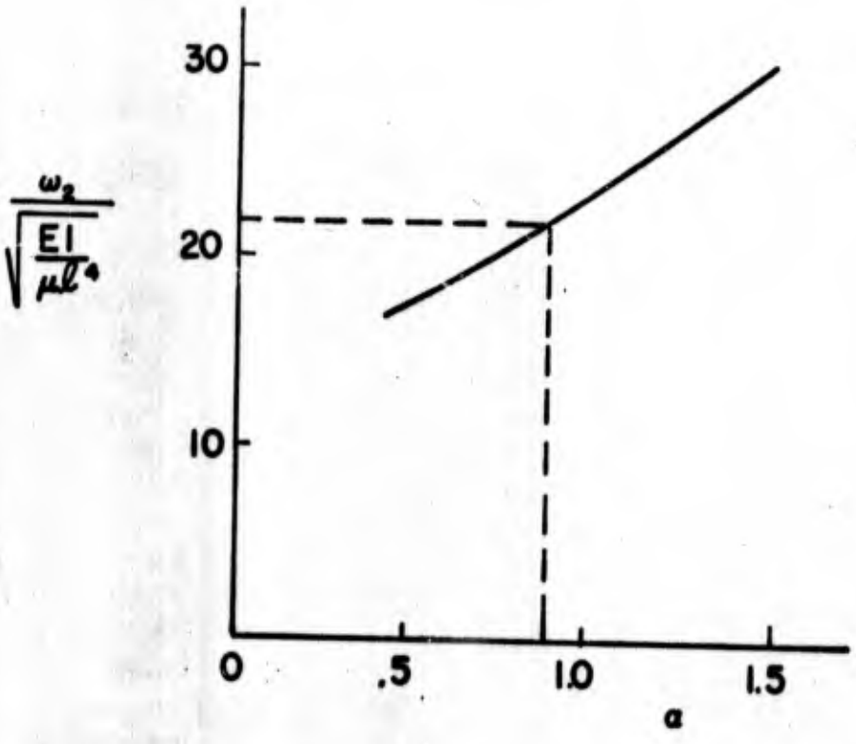

FIG. C- 3(d) SECOND NATURAL FREQUENCY VS, α
TWO MASS, CLAMPED- FREE BEAM

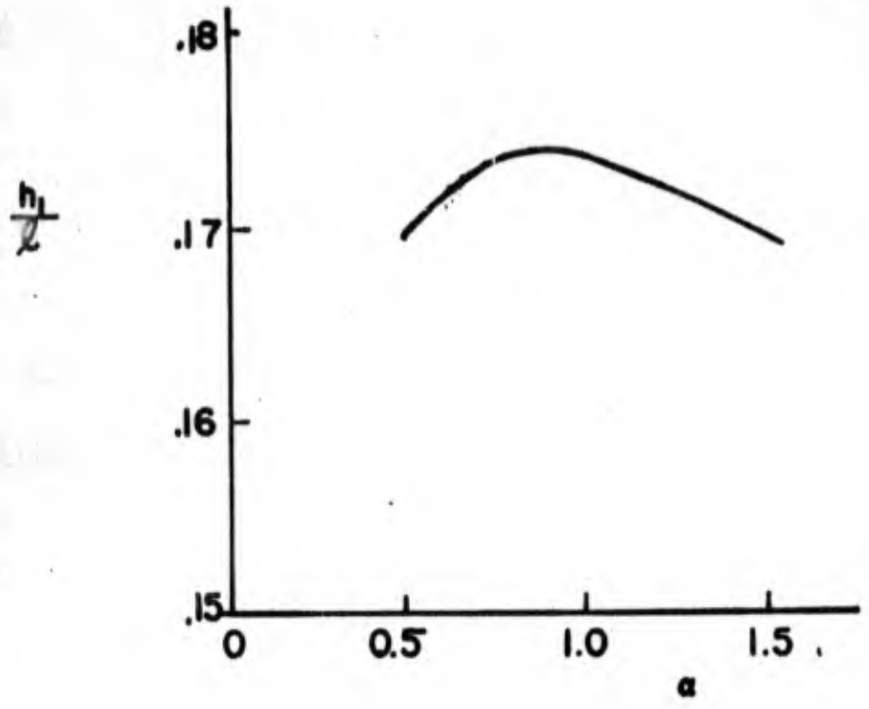

FIG. C-4(d) POSITION OF MASS m_1 VS. α
THREE MASS, HINGED-HINGED BEAM

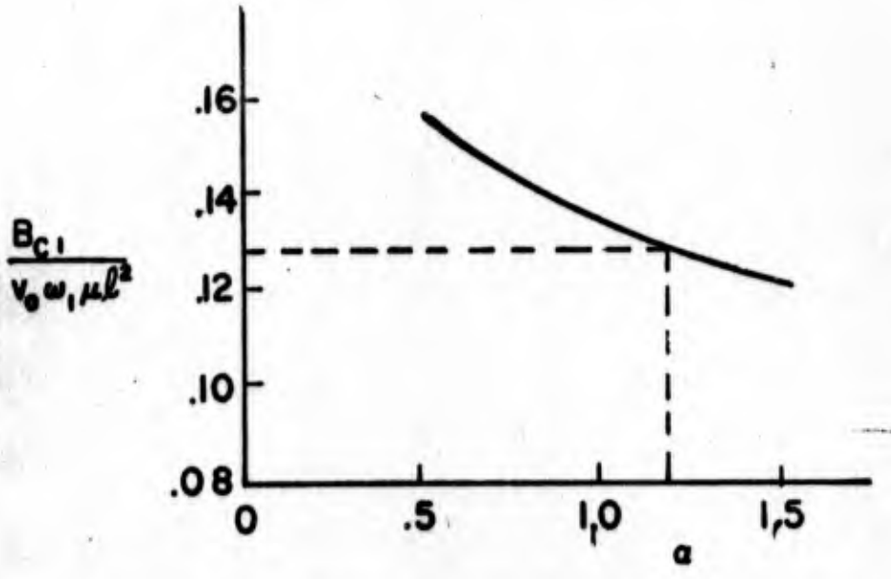

FIG. C-4(b) FIRST MODE BENDING MOMENT VS. α
THREE MASS, HINGED-HINGED BEAM

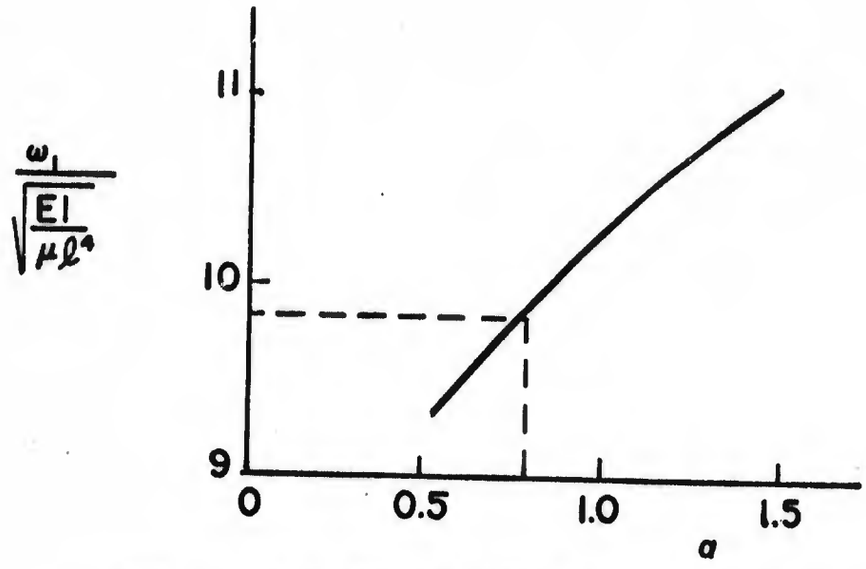

FIG.- C-4(c) FIRST NATURAL FREQUENCY VS. α

THREE MASS, HINGED-HINGED BEAM

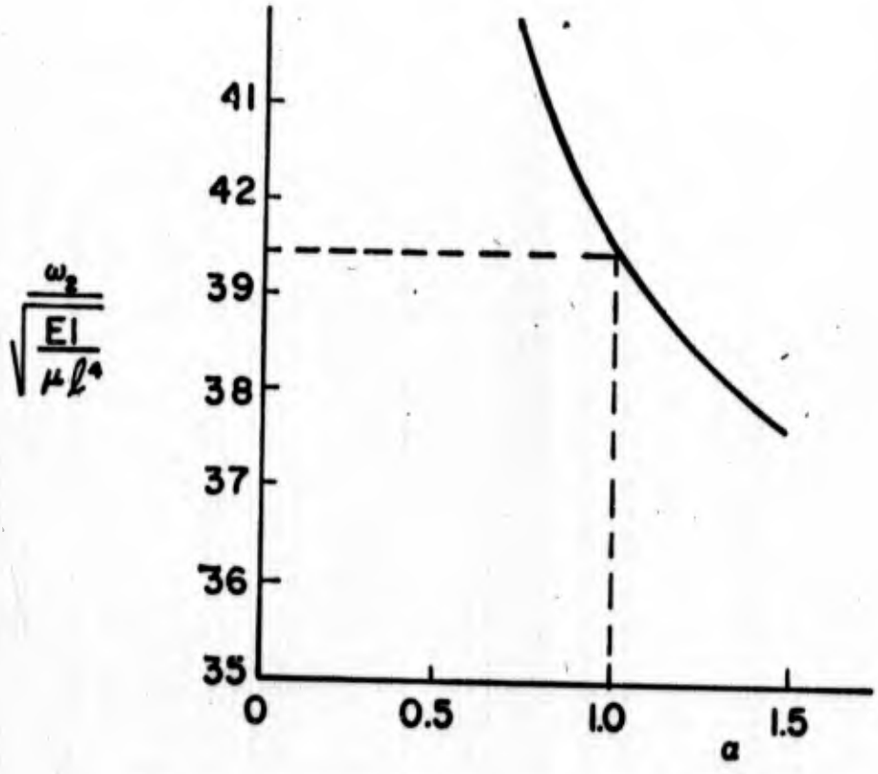

FIG. C-4(d) SECOND NATURAL FREQUENCY VS. α

THREE MASS, HINGED-HINGED BEAM

References

1. Neubert, V.H., "Shock Analysis of Structural Networks," Office of Naval Research, Contract No. Nonr-656(28)(x), Interim Report No. 1, February 1964.

2. Neubert, V.H. and Lee, Hae, "Shock Analysis of Structural Networks," Office of Naval Research, Contract No. Nonr-656(28)(x), Interim Report No. 2, February 1965.

3. Neubert, V.H., "Series Solutions for Structural Mobility," Journal of the Acoustical Society of America, Vol. 38, No. 5, pp. 867-876, November 1965.

4. Neubert, V.H. and Lee, Hae, "Shock Analysis of Structural Networks," Office of Naval Research, Contract No. Nonr-656(28)(x), Interim Report No. 4, February 1966.

5. Lee, Hae, "Optimum Modelling of Structures to Predict Dynamic Elastic Response," Ph.D. Thesis, Department of Engineering Mechanics, 1966.

6. Mindlin, R.D. and Goodman, L.E., "Beam Vibrations with Time-Dependent Boundary Conditions," J. Appl. Mechanics, pp. 377-380, 1950.

7. Felgar, R.P. Jr., "Formulas for Integrals Containing Characteristic Functions of a Vibrating Beam," Circular No. 14, University of Texas, Austin, Texas, 1950.

8. Young, D. and Felgar, R.P. Jr., "Tables of Characteristic Functions REpresenting Normal Modes of Vibration of a Beam," No. 4913, The University of Texas, Austin, Texas, 1949.

9. Archer, J.S., "Consistent Mass Matrix for Distributed Mass Systems," Proc. Am. Soc. Civil Engineers, 89, ST4, pp. 161-178, August 1963.

10. Leckie, F.A. and Lindberg, G.M., "The Effect of Lumped Parameters on Beam Frequencies," The Aeronautical Quarterly, pp. 224-240, August 1963.

11. Neubert, V.H., "Lumping of Mass in Calculating Vibration Response," Jrl. of Eng. Mech. Div., ASCE, Vol. 90, No. EM-1, February 1964, pp. 47=67.

12. Belsheim, R.O. and O'Hara, G.J., "Shock Design of Shipboard Equipment, Part I - Dynamic Design - Analysis Method," NRL Report 5545, U.S. Naval Research Laboratory, Washington, D.C., September 16, 1960.

Unclassified

Security Classification

DOCUMENT CONTROL DATA - R&D

(Security classification of title, body of abstract and indexing annotation must be entered when the overall report is classified)

1. ORIGINATING ACTIVITY (Corporate author)	2a. REPORT SECURITY CLASSIFICATION
The Pennsylvania State University	Unclassified
	2b. GROUP NA

3. REPORT TITLE

Lumped Parameter Beam Models Based on Mechanical Impedance

4. DESCRIPTIVE NOTES (Type of report and inclusive dates)

Interim Report No. 6 (March 1966 through February 1967)

5. AUTHOR(S) (Last name, first name, initial)

Neubert, Vernon H.

Lee, Hae

6. REPORT DATE	7a. TOTAL NO. OF PAGES	7b. NO. OF REFS
February 1967	55	12

8a. CONTRACT OR GRANT NO.	9a. ORIGINATOR'S REPORT NUMBER(S)
Nonr-656(28)(X)	Interim Report No. 6
b. PROJECT NO.	
c.	9b. OTHER REPORT NO(S) (Any other numbers that may be assigned this report)
d.	N.A.

10. AVAILABILITY/LIMITATION NOTICES

Qualified requesters may obtain copies of this report from DDC.

11. SUPPLEMENTARY NOTES	12. SPONSORING MILITARY ACTIVITY
None	Office of Naval Research Naval Research Laboratory, Code 6260 Washington 25, D.C.

13. ABSTRACT

A new approach has been used, based on an impedance method, to develop accurate lumped parameter models of uniform Bernoulli-Euler beams. By adjusting the parameters so that the impedance of the models is accurate at the boundaries, it is demonstrated that they will also be accurate for ground shock loading if the spectrum of the loading indicates low frequency content. Improved models for clamped-clamped, hinged-hinged, clamped-free, clamped-propped, and clamped-guided beams are presented. Some previous results for bars are summarized. Also some previous results based on matching modal parameters are included, so that the report summarizes most of the work by the authors to date.

14. Key Words

Shock, Vibrations, Impedance, Mobility, Structural Networks, Bars, Beams.

DD FORM 1 JAN 64 1473

Unclassified

Security Classification